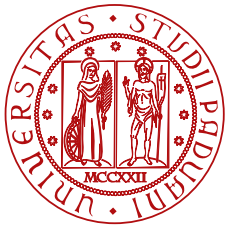

UNIVERSITÀ DEGLI STUDI DI PADOVA

DIPARTIMENTO DI INGEGNERIA DELL'INFORMAZIONE

DIPARTIMENTO DI INGEGNERIA DELL'INFORMAZIONE
MASTER THESIS/ CORSO DI LAUREA MAGISTRALE IN
ICT for Internet and Multimedia

Analysis of lateralization of brain dopamine function in psychosis: [18F]FDOPA PET imaging study

MASTER CANDIDATE/LAUREANDO

Fatima Rabia YAPICIOGLU

Student ID 2049536

SUPERVISOR/RELATORE

Prof. Mattia Veronese

University of Padova, Italy

CO-SUPERVISOR/CORRELATORE

Alessio Giacomel, MsC

Giovanna Nordio, PhD

Kings College, London

ACADEMIC YEAR/ ANNO ACCADEMICO 2022/2023
DATE OF GRADUATION/ DATA DI LAUREA 13/07/2023

To my parents Yilmaz Yapicioglu & Fahriye Yapicioglu and my sister Eda Yapicioglu for their faith, patience, and support.

To our beloved family fellow and lawyer Güner Car for his support and advice.

To my Prof. Leonardo Badia for introducing the University of Padova and the department to me initially.

To the Ministry of Foreign Affairs and International Cooperation of Italy for providing me with the prestigious national MAECI scholarship for two consecutive years.

To Mustafa Kemal Atatürk, founder of the Republic of Turkey and who has the fundamental tenet of 'The supreme guide in life is science'.

Abstract

Abnormal dopamine brain function is a hallmark of psychotic disorders like schizophrenia, and the main pharmacological target for psychotic treatment. However, the functional organization and regulation of the dopamine system are not completely known, due to its complex topology and interplay with other neuroreceptor systems. The primary objective of this research is to comprehend the normal state of dopamine lateralization in the human brain and identify whether dopamine lateralization is altered in schizophrenia. This study considered a dataset of 136 patients with psychosis matched to 143 healthy controls acquired with the $[^{18}F]FDOPA$ PET imaging, a biomarker for measuring dopamine synthesis capacity in vivo in humans. For each subject, neuroimaging metrics from 41 regions of interest (ROIs) were derived using the Desikan-Killiany atlas for each brain hemisphere. For each ROI and each subject, a lateralization index (lx) was computed to compare the dopamine function between the left and right hemispheres. The same metrics were fed into the Random Forest, XGBoost, SVM, KNN, Naïve Bayes, and Logistic Regression classifier models to distinguish patients and controls by exploiting the difference with the best-performing model in brain dopamine lateralization. In normal individuals, brain dopamine is mainly lateralized in the Inferior Parietal (p=0.039) and Transverse Temporal (p=0.004) with a significant effect of age and gender. Moreover, when comparing lateralization between controls and patients, left-biased lateralization in Putamen decreases 50%, right-biased lateralization in Accumbens decreases 60%, and right-biased lateralization in Pallidum changes direction and shows a significant increase around 300% in Ki levels. In terms of patient classification, the best performing model was XGBoost with the metrics of 79% accuracy, 79% precision, 79% recall, and 78% f1-score on the test set. Finally, the post hoc model agnostic explainability method SHAP reported the Accumbens, Fusiform, Posterior Cingulate, Thalamus, and Pallidum as the top 5 most salient features which have a significant effect on the decision. In conclusion, healthy controls present a clear lateralization of dopamine function that can change its direction and magnitude in the case of schizophrenia. Further studies should focus to investigate the biological rationale behind these differences and their implication for the stratification of patients with psychosis.

Contents

List of Figures

List of Tables

List of Acronyms

HC Healthy Controls

XAI Explainable Artificial Intelligence

KNN K-nearest Neighbours

SVM Support Vector Machine

LIME Locally Interpretable Model Agnostic Explanations

ROI Region of Interest

SHAP Shapley Additive Explanations

PET Positron Emission Tomography

1

Introduction

This research provides extensive data analysis and modeling to understand the links between the topology of brain dopamine function and schizophrenia with psychotic symptoms, by investigating differences in lateralization between healthy controls and patients using $[^{18}F]FDOPA$ PET imaging.

Dopamine is a neurotransmitter that is highly involved in the regulation of motivation, cognitive functions, and control of movement in humans. This molecule is mostly produced by the brain's substantia nigra, the ventral tegmental area (VTA), and the hypothalamus and is correlated with mechanisms of addiction, reinforcement, and reward (Arias-Carrión and Pöppel 2007). Neurological and behavioral problems caused by dopamine system dysfunction are related to anomalies in brain dopamine levels in certain regions and lateralization (Olguín et al. 2016). Any form of reward triggers an increase in dopamine transmission, as do numerous medications with strong addictive properties (Wise and Robble 2020). Furthermore, due to its close association with neurological and psychiatric disorders, dopamine is a prominent topic in neuroscience research and a key molecular target in pharmacological research.

Psychosis refers to a broad range of psychiatric disorders that causes a person to lose touch with reality such as visual and auditory hallucinations, disorganized thoughts, and unexpected behaviors. Moreover, Schizophrenia, a neurodegenerative disorder with unclear etiology, is mostly characterized by psychotic symptoms. Based on the fact that dopamine-releasing medications can cause Psychosis, Schizophrenia was once thought to be a "dopamine illness" (Insel 2010). To understand dopaminergic impairment and associated pathol-

ogy, it is necessary to understand the dopamine function of the healthy population's brain organization and condition in terms of lateralization, as well as the change in dopamine function in the Schizophrenia patients cohort with psychosis symptoms.

In this chapter, we provide explanatory information including dopamine hormone, neurodegenerative disorders, Schizophrenia, psychotic symptoms, data analysis, and explainable artificial intelligence. Subsequent sections introduce methodologies in detail, and finally, outcomes of the research are provided in results, and conclusions are discussed in detail in the last section.

1.1 Psychosis Symptoms and Schizophrenia

Schizophrenia is a neurodegenerative disorder that presents with psychotic symptoms such as hallucinations and delusions, inattentiveness, and overall difficulties with cognitive capabilities (Picchioni and Murray 2007). Global estimates of the prevalence of Schizophrenia in non-institutionalized individuals range from 33% to 75% (Moreno-Küstner, Martin, and Pastor 2018). Additionally, systematic analyses show that Schizophrenia has a high prevalence (7.2/1000 people) but a low incidence (15.2/100,000 people), possibly because it often manifests in early adulthood and develops into a chronic illness. Schizophrenia was ranked among the top 15 global reasons for disability in 2016 (Saha et al. 2005; Hay et al. 2017). Also, early adulthood or late youth are the common times when Schizophrenia initially manifests its symptoms (Lichtenstein et al. 2009). Considering the gender differences, men were diagnosed on average earlier than women (34.4 ± 12.6 years) (I. E. Sommer et al. 2020). Moreover, up to 80% of Schizophrenia cases are thought to be heritable (Hilker et al. 2018). After a century of research and a concentration on brain chemistry in the second half of the 20th century, the etiology of Schizophrenia has not been identified. In comparison to the general population, Schizophrenic patients often have a 22-fold higher lifetime risk of dying by suicide, a 15-year shorter life expectancy, and lower reproductive rates (Hjorthøj et al. 2017). One of the accepted theories elucidating the causes of this disease is an alteration of the dopaminergic pathways and system (Soares and Innis 1999; Hietala, Syvälahti, Vilkman, et al. 1999).

1.2 Dopamine and $[^{18}F]FDOPA$ PET imaging

Dopamine is essential for the regulation and control of movement, motivation, and cognition. It is also linked to motivation, reinforcement, and addiction. Dopamine deficiencies in the brain have been linked to a variety of neurological and psychiatric disorders, including Schizophrenia. The various cluster of symptoms of the condition has been hypothesized to be caused by both an increase and a decrease in dopamine function (Elkashef et al. 2000).

PET imaging is a technique used to track the spatial variability and kinetics of bioactive compounds labeled with positron-emitting isotopes in the human organism (Fowler and Wolf 1989). PET allows for the precise measurement of dopamine system components in the living human brain. It is based on radiotracers that recognize dopamine receptors, dopamine transporters, dopamine precursors, or compounds that have specificity for the excreting dopamine. PET dopamine measurements were employed to study the healthy brain as well as its role in psychiatric and neurodegenerative disorders (Volkow et al. 1996).

These findings support the development of the short $[^{18}F]FDOPA$ scan as a pathophysiologically relevant biomarker to direct therapy choice for patients with psychosis. It was demonstrated by Veronese et al. that $[^{18}F]FDOPA$ PET imaging protocol provides reliable and reproducible measures of dopamine synthesis (Veronese et al. 2021). Additionally, it was shown that in PET Schizophrenic patients' dopaminergic lateralization is abnormal when compared to that of healthy individuals with a PET study (Farde et al. 1990). Furthermore, there were several other research in the literature which focus on the lateralization of specific structures with $[^{18}F]FDOPA$. It was applied to research primary brain tumor molecular imaging (Calabria et al. 2012), Parkinson's disease (Morrish, Sawle, and Brooks 1996; Morrish, Sawle, and Brooks 1996), and various tumors (Hoegerle et al. 2001) and malignancies (Ismail and Hussain 2010).

1.3 Brain Asymmetry and Lateralization in Schizophrenia

The brain of a healthy individual has significant asymmetry in both its functional metabolism and physical architecture. Molecular and functional imaging techniques reveal evidence of lateralization of human cerebral structure and

function of the healthy brain (Toga and Thompson 2003; Rentería 2012).

A wide variety of brain regions exhibit structural hemispheric asymmetries, which are anatomical disparities between the two sides of the brain (such as variances in the volume or size of a particular area)(Ocklenburg and Güntürkün 2012). This is true in physiological conditions as well as in disease as Schizophrenia. For example, a study revealed that compared to the control group, the mean gray- and white-matter volumes were considerably lower in the Schizophrenia group (Takao et al. 2010). Another structural asymmetry study shows that in comparison to the control participants, the left Sylvian fissure length was considerably shorter in the Schizophrenia group (p=0.0001), whereas the right Sylvian fissure length remained constant (Falkai et al. 1992). Additionally, compared to both healthy controls and psychiatric patients, the prevalence of mixed- and left-handedness was considerably higher in patients with Schizophrenia. (I. Sommer et al. 2001). Prior research showed that people with Schizophrenia had less laterality than controls without Schizophrenia regarding less left gray matter volume (DeRamus et al. 2020). Furthermore, a study reported that when compared to patients with first-episode affective Psychosis or healthy control subjects, patients with first-episode Schizophrenia displayed significant alterations in gray matter volume over time in the left superior temporal lobe (Ortelli et al. 2018). Another study discovered that patients' left Anterior Superior Temporal Gyrus was considerably smaller and that the volume of this area was inversely linked with the intensity of hallucinations (Barta et al. 1990). Concerning cortical thickness, it has been reported that the frontal and temporal regions of the brain exhibit the most extreme thinning over the course of Schizophrenia, although this excessive thinning affects many other parts of the brain (Van Haren et al. 2011).

A growing body of research also showed that Schizophrenia has reduced asymmetry of the brain that is not only structural (Friston 2002; Koch et al. 2008; Ribolsi et al. 2009; Baker et al. 2014; Zhang et al. 2015) but also functional due to abnormal asymmetry of functional connections in comparison to healthy subjects (Jalili et al. 2010).

There is no evidence of lateralization of dopamine function in Schizophrenia. However, a few studies investigated the dopamine system in Parkinson's disease (PD), a brain disorder that is as Schizophrenia and is characterized by dopamine function alterations. Specifically, the attentional functions may be impacted by the asymmetrical degradation of the dopaminergic system (Ortelli et al. 2018). Another study found that the course of PD is affected by hemispheric asym-

metric dopaminergic degenerative changes. Greater motor severity is related to dominant right hemispheric nigrostriatal dopaminergic loss, but the onset and course of cognitive symptoms are affected by more pronounced left hemispheric denervation (Fiorenzato et al. 2021).

1.4 Exploratory Data Analysis and Statistics

A thorough understanding of the structure of analyzed data enables the formulation of detailed scientific theories and research questions. Practices for exploratory data analysis can reveal the data structure and basic relationships between parameters in the data. Furthermore, data visualization is a critical component of data exploration analysis. It enables us to connect facts and draw conclusions based on the results of previous steps in the analysis (Cangür, Sungur, and Ankarali 2018). On the other hand, taking the non-normally distributed structure of the data belonging to our research, we had to reference non-parametric methods such as Quades' Non-Parametric ANCOVA (Quade 1967). Thereafter, we extended the analysis results with detailed plots with Python visualization libraries and Brain Painter by MIT (R. V. Marinescu et al. 2019).

1.5 Explainable Artificial Intelligence (XAI)

In the field of health care, artificial intelligence (AI) has expanded to a number of applications, including patient data and diagnosis, clinical decision-making, management of health services, and predictive medicine. While performing at a level comparable to humans, AI models still have a limited range of applications since they are regarded as a mystery. Their poor utilization in practice, particularly in healthcare, continues to be caused mostly by this lack of trust. In order to encourage the use of AI systems in healthcare, explainable artificial intelligence (XAI) has been developed as a technique that can boost user confidence in a model's prediction by outlining how it was made (Loh et al. 2022).

Given the information above, it is crucial to use a suitable explainability method to better comprehend the captured pattern by examining which elements are the most important decision-makers. LIME (Local Interpretable Model-agnostic Explanations) is one of the suitable ways to determine which ROIs have the most significant impact on the classification choice produced by the classi-

fier, taking into account the requirements of age, gender, and instance-based unique lateralization values. By building an interpretable model locally around the prediction, LIME presents a revolutionary explanation technique that explains the predictions of any classifier in an understandable and accurate manner (Ribeiro, Singh, and Guestrin 2016). Moreover, using the game's theoretically ideal Shapley values, Lundberg and Lee developed SHAP (Shapley Additive Explanations), a technique to explain specific predictions (Lundberg and Lee 2017).

Even though LIME is a model-agnostic interpretability method, the XGBoost (Extreme Gradient Boosting) (T. Chen and Guestrin 2016b) was referenced. XGBoost, contrary to numerous other algorithms, is an ensemble learning algorithm (Mohammed and Kora 2023), which means it combines the results of many models, known as base learners, to make a prediction. To employ the XGBoost model for our research, we considered lateralization indices as features and diagnosis labels, healthy controls, and patients, as output, the model provides insights into underlying patterns of how Schizophrenia patients' lateralization changes.

1.6 Problem Statement and Research Objectives

Taking into account the aforementioned information, we were interested in revealing the difference between healthy controls (N=143) and patients' (N=136) dopamine function lateralization using the $[^{18}F]FDOPA$ imaging method thorough data analysis of locations in the Desikan-Killiany(DK) atlas and verifying the results with an XAI-guided XBoost model classifier. Due to the interplay between psychosis symptoms and dopamine, we aim to provide comprehensive data analysis and reveal the different states of brain lateralization organization between healthy controls and Schizophrenia patients, paving the way for a robust diagnosis and cutting-edge therapeutic approaches.

Moreover, we extend the exploratory data analysis with new machine learning (ML)-based decision-support framework to identify brain topological features associated with Schizophrenia. Through the use of machine learning, systems may learn from data and their past performance. The learning process begins with the available data and develops on its own over time. Furthermore, the explainable artificial intelligence (XAI) techniques are providing users with global and local explainability algorithms to unpack black-box machine learning

models and extract the most salient features that have a significant effect on the decision. To identify novel disorder-related brain patterns, recent developments in machine learning may now evaluate discrepancies in the local morphological characteristics of different brain subregions (Bose et al. 2008; Greenstein et al. 2012; Libero et al. 2015; Orru et al. 2012).

Previous works in molecular neuroimaging showed that aberrant pre-synaptic dopamine density in individuals with Schizophrenic psychosis was mainly lateralized to the left and that patients had a substantial left rise of striatal D_2 receptors (Hietala, Syvälahti, Vuorio, et al. 1995). Given this evidence, it is conceivable to hypothesize that differential lateralization of dopamine function is present in psychosis compared to normal brain functioning.

Moreover, in previous works on neuroimaging ML works in psychosis, dopamine (as measured by FDOPA PET) was employed to assess treatment response to antipsychotic medication. In the work, the authors tested linear and non-linear methods and selected as the best-predicting model a linear SVM (AUC=0.89) using as feature striatal dopamine synthesis capacity (Veronese et al. 2021). Even though the prior research achieved relatively good accuracy, the sole models do not provide justifications and explanations for their decisions to proceed with the developments in stratification studies, lacking interpretability. Moreover, highly predictive models, on the other hand, are typically complicated and hard to interpret (Katuwal and R. Chen 2016).

However, the traditional statistical approaches and linearity assumptions of data might be a limitation to further discoveries on focal ROIs that trigger the illness, limitations that could be mitigated by more data-driven machine learning (ML) approaches.

The overall objectives and novel contributions of this research can be listed as follows:

- Identifying the dopamine brain synthesis lateralization in healthy controls and investigating the presence of differences in Schizophrenia patients.
- Determining the focal ROIs that have been distributed significantly differently considering $[^{18}F]FDOPA$ dopamine synthesis measures
- Developing and comparing the performance of different classifier models that have been trained with $[^{18}F]FDOPA$ PET imaging of all ROIs with the aim of differentiating between healthy controls and Schizophrenia patients.
- Verifying and assessing the nominated ROIs constituting the difference between healthy controls and patients with XAI methods and statistics.

2

Materials and Methods

2.1 Dataset

$[^{18}F]FDOPA$ from 142 Healthy Controls (HC) and 136 patients affected by psychosis from previously published studies were included in the study. Patient data included both responders (N=71) and non-responders (N=65) to standard anti-psychotic treatment, as measured at follow-up after 6 weeks of treatment. Age information of the healthy controls was aligned between 19 - 54, and the mean age is 28.3 and the standard deviation was 7.7. On the other hand, the age information belonging to patients' data including both responders and non-responders was between 18 - 65, and the mean age was 32 along with a standard deviation of 10.7. Data were collected in three different imaging centers (Imanet, London; Invicro, London and South Korea) using a total of 5 different scanners (Siemens Hi-Rez Biograph 6, Siemens Biograph 40 TruePoint, Siemens TruePoint 6, ECAT HR+ 962 and ECAT EXACT 3D). To remove the technological effects of the scanner, imaging content was harmonized using Combat Harmonization (Orlhac et al. 2022), using age and sex as covariates for which the variance has to be preserved. All data were collected with the same $[^{18}F]FDOPA$ imaging protocol and all data were quantified with the same in-house developed Python pipeline (Nordio et al. 2023). In brief, the K_i^{cer} parameter (also referred to as $K_i[1/min]$) was estimated using Gjedde-Patlak graphical method using the cerebellum as a low-binding region (reference region) and normalized to MNI152 standard space (Linear n.d.).

Finally, for our analysis average values were extracted from regions of the

Desikan-Killiany (DK) atlas (Desikan et al. 2006), composed of 82 bilateral regions (41 for the left hemisphere and 41 for the right hemisphere) and one region of the brainstem. Considering that data balance plays a significant role in both statistical calculations and model training, we outlined the samples belonging to cohorts of healthy controls and patients close in terms of sample numbers. Lateralization indices have been calculated and then added to the main data frame. All operations belonging to the data preparation and analysis were implemented in the Jupyter Lab environment with Python 3.8, and IBM Statistics SPSS.

2.1.1 Data Preprocessing

The laterality index (LX) is one method for assessing hemispheric dominance in a variety of regions and providing information on how laterality changes with factors such as age, gender, and different cohorts. To calculate lateralization indices, we used the following formula:

$$L_x^{ROI} = \frac{(L^{ROI} - R^{ROI})}{(L^{ROI} + R^{ROI})}$$

where L^{ROI} and R^{ROI} indicate the average K_i values belong to the left hemisphere and right hemisphere respectively. Before feeding K_i values to the above formula, we handled the negative K_i values with a normalization approach that references the idea that rounding up negative values to zero and leaving positive values as original. Moreover, we can interpret the lateralization bias easily according to the positive or negative sign. If the resulting value for L_x^{ROI} index is positive ($L^{ROI} > R^{ROI}$), it means that the associated lateralization is leftwards. If the resulting value for L_x^{ROI} index is negative ($R^{ROI} > L^{ROI}$), it means that the associated lateralization is rightwards.

Due to the normalization requirement of negative Ki values, we proposed an approach that references rounding negative values to 0 and leaving positive ones as their original. Following the normalization, we calculated lateralization indices and then again normalized these values between -1 and 1. Furthermore, it is customary to normalize the data prior to training machine learning models on it in order to potentially achieve better, quicker outcomes. Additionally, normalization reduces the sensitivity of the training process to the scale of the features, producing better coefficients following training and better results for

statistical analysis.

2.2 Analysis

The majority of the analysis was implemented on the Jupyter Lab environment by using Python 3.8 with the libraries of Matplotlib, Seaborn, Numpy, Pandas, LIME, Scipy, and StatsModels, and IBM Statistics SPSS was used for Quade's test.

To study the Ki differences between the left and right hemispheres in each ROI, first, we investigated the absolute difference in Ki levels between the left and right. Alternatively, we applied the Wilcoxon Signed-Rank test which is a non-parametric equivalent to the dependent t-test. The Wilcoxon test was used on a cohort of healthy controls to reveal baseline lateralization and which ROIs have significantly different Ki-level distributions between the left and right hemispheres. At this point, we also calculated lateralization indices for all ROIs and included them in the main dataset. Further, the outcoming ROIs from the Wilcoxon test went under the Quades' Non-Parametric ANCOVA test to search for the gender factor by taking also the age factor into consideration. Thereafter, to search for age and lateralization relationship simple linear regression was applied to outcoming ROIs of the Wilcoxon test. Thus, we outlined how lateralization changes with age and gender factors in detail as a result of simple linear regression and Quades' Non-Parametric ANCOVA.

Having had the knowledge of how brain dopamine is lateralized in healthy controls cohort, we extended research to investigate the differences between patients and healthy controls in terms of brain dopamine lateralization. In this regard, we compiled a dataset that consists of both cohorts to apply Quades' Non-Parametric ANCOVA. During the second Non-Parametric ANCOVA age and gender factors were set as covariates and cohort was set as the grouping factor. Thus, we revealed the ROIs that are following significantly different lateralization indices between healthy controls and patients. Moreover, the lateralization value differences between the healthy controls and patients were visualized via the tool BrainPainter (R. Marinescu et al. 2019).

Finally, diverse machine learning classifier models were built to differentiate between healthy controls and patients with an explainable artificial intelligence (XAI) approach to reveal ROIs that have a significant effect on the decision made by the classifier.

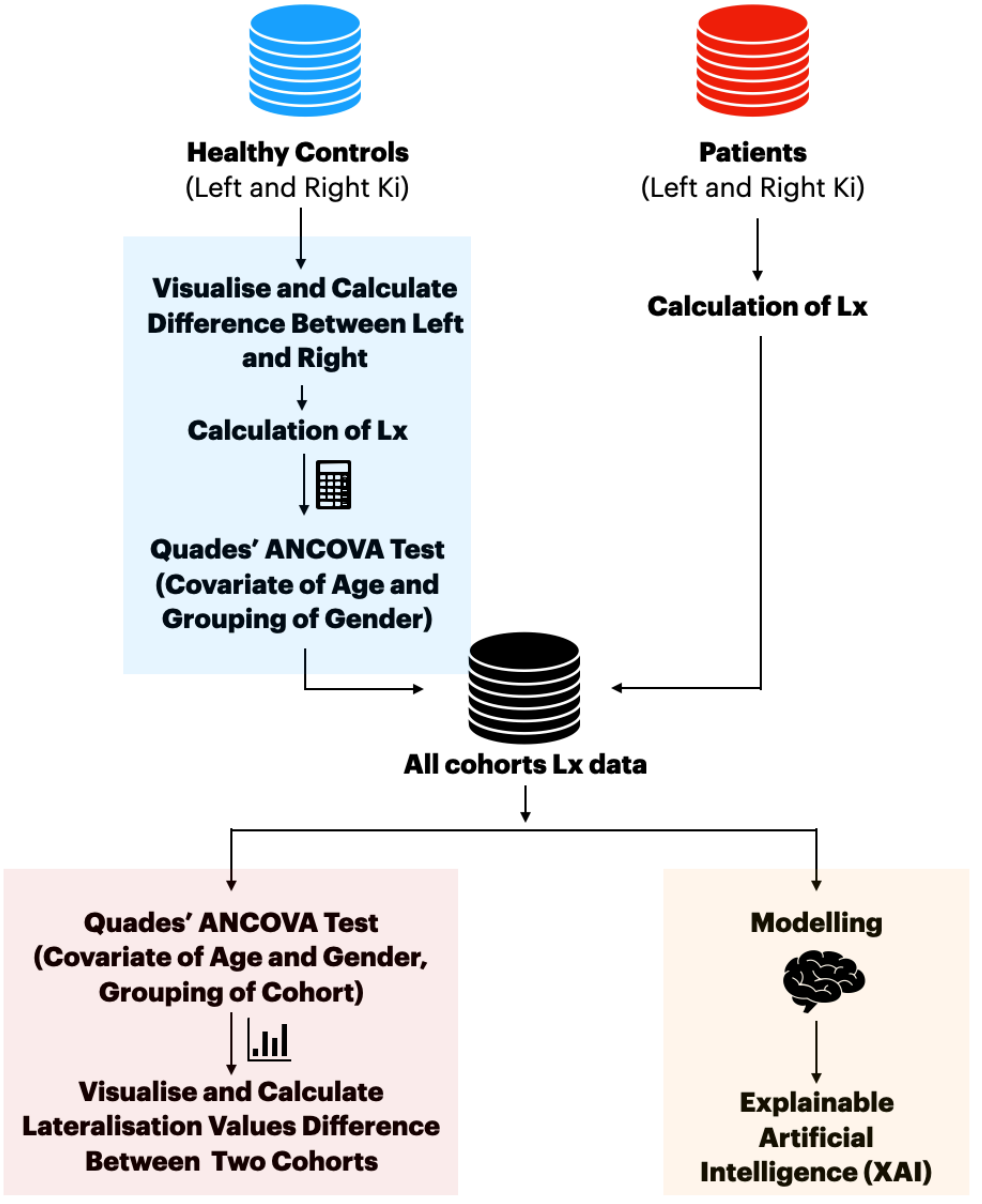

Figure 2.1: The Complete Analysis Map

As illustrated in Figure 2.1, the blue lane includes the steps aiming to understand dopamine lateralization in healthy controls. The red lane compromises the steps for revealing the differences in dopamine lateralization between healthy controls and patients. Finally, the yellow lane contains artificial intelligence and explainability research.

2.2.1 Wilcoxon Signed-Rank Test

The Wilcoxon signed-rank test non-parametric test is a statistical hypothesis test that can be used to test the location of a population using a sample of data or to make a comparison of the locations of groups using two matched samples (Conover 1999). Since the Wilcoxon signed-rank test does not require data to be normally distributed, it can be used when this assumption can not be held and the dependent t-test is inappropriate. It is used to evaluate and compare two groups of test results from the same individuals participating.

A summary of the Wilcoxon Test algorithm can be found as follows:

- Determine the differences in the measurement values.
- Sort the differences and allocate a rank to each one.
- Get the absolute value if the difference becomes negative. In the case of a tie, compute the average rank.
- Calculate the sum of the ranked negative and positive differences.
- Determine the critical value using a Table of Critical Values for W and the Wilcoxon (W) test statistic. The W-statistic is calculated by taking the absolute value of the smaller of the two sums.

We focused on only the healthy controls cohort to reveal the baseline brain dopamine lateralization and organization between the left and right hemispheres.

2.2.2 ANOVA and ANCOVA

To investigate lateralization index trend in more detail along with the knowledge of age and gender, we experimented with Quade's Non-Parametric ANCOVA. The Quade method is based on comparing the residuals obtained from the linear regression of the ranked dependent variables and the ranked covariate between cohorts (Quade 1967; Cangür, Sungur, and Ankarali 2018).

The quade method has been applied to outcoming ROIs that have been reported as significant by the Wilcoxon test and also to the outcoming ROIs where

the Wilcoxon test was applied to data with all cohorts. Thereafter, the number of ROIs that have been showing significant differences by taking the age, gender, and cohort information into consideration is reduced.

2.2.3 Simple Linear Regression

Simple linear regression analysis is a significant statistical technique for analyzing medical data. It allows for the identification and characterization of relationships between various factors. Scikit learn linear regression package (Pedregosa et al. 2011). which uses Python was referenced. The regression analysis has been used the evaluate how the lateralization changes with the age factor or in close correlation with it.

2.2.4 XGBoost Classifier Model

XGBoost, which stands for 'Extreme Gradient Boosting,' is a supervised and powerful machine learning algorithm. It is based on ensemble learning principles, employing multiple decision tree structures and boosting, which is a sequential process in which each subsequent model tries to correct the mistakes of the previous model. It also has numerous benefits such as regularization to avoid overfitting, handling sparse data, and being explainable by design.

The boosting technique which is provided in Figure 2.2 provides weak learners with low prediction performance who perform moderately better than random guesses with a particular weighted subset of the original data. Subsets that were previously misclassified are given more weight. In the case of classification, classifiers are merged with voting mechanisms to align with our research. Furthermore, gradient boosting generalizes by using differentiable function losses from weak classifier models as in the following formula:

$$F_{x_{t+1}} = F_{x_t} + \epsilon_{x_t} \frac{\partial f}{\partial x}(x_t)$$

The learners are used at each boosting phase to minimize the loss function based on the current model. As we iterate over the model, the loss function will converge to a minimum value that it could be.

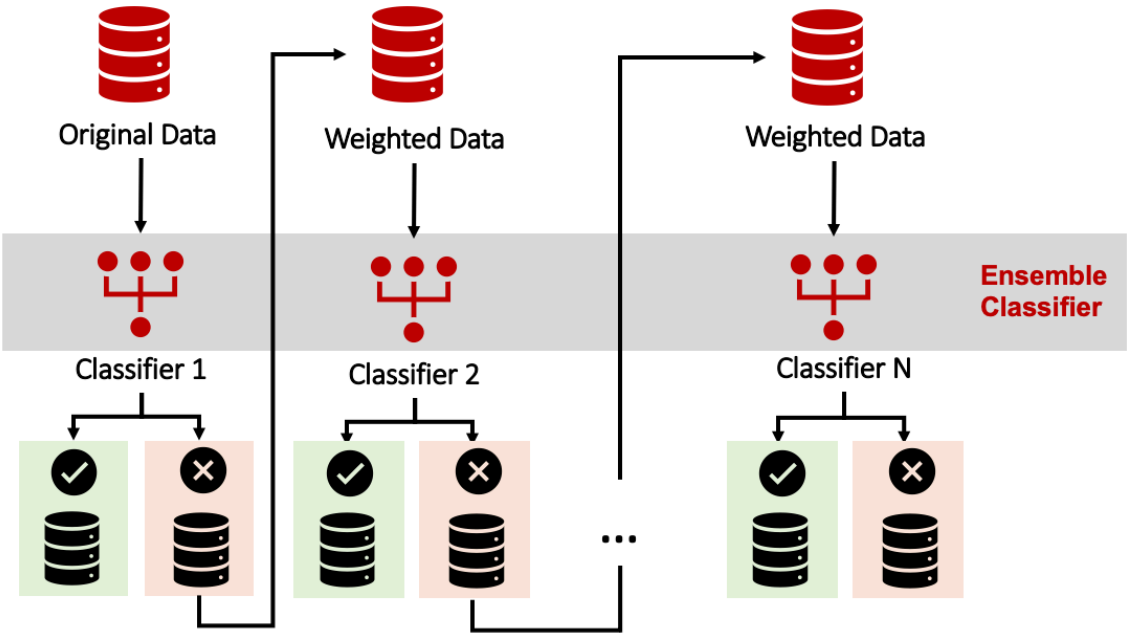

Figure 2.2: Implementation of a boosting algorithm

2.2.5 Random Forest Classifier

Random forest is another supervised machine learning algorithm that can be used for both regression and classification. An ensemble of decision trees, often trained using the bagging approach, make up the "forest" that it constructs. The bagging method's main premise is that combining learning models improves the end outcome. Instead of depending on a single decision tree, the random forest uses forecasts from all of the trees to anticipate the outcome based on which predictions received the most votes.

As illustrated in Figure 2.3, bagging references the concept of merging homogenous weak learners' models that learn concurrently and independently from one another. However, in Boosting, models learn progressively and adaptively to enhance the complete model predictions. While the model XGBoost references the concept of boosting, the Random Forest model references the concept of bagging.

2.2.6 K-Nearest Neighbours (KNN)

KNN is a non-parametric, supervised learning algorithm (Guo et al. 2003) that can be used for both classification and regression. As illustrated in Figure

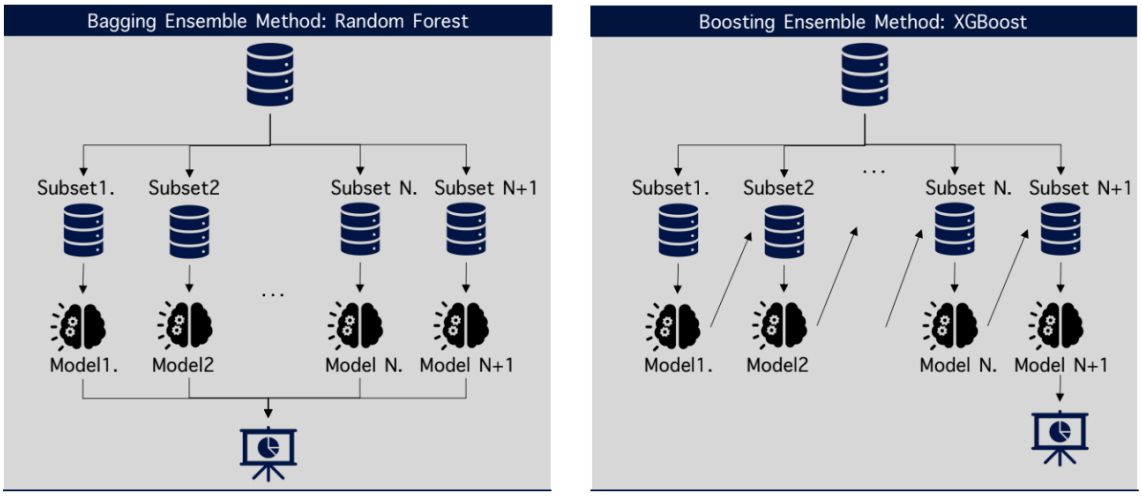

Figure 2.3: Bagging vs Boosting

2.4, the k-nearest neighbors technique employs proximity to classify or anticipate how a single data point will be grouped. The number of nearest points taken into account for classification is indicated by the parameter k in kNN. The total amount of these points needed to calculate the outcome is indicated by the value of k. It will be necessary to compute the distance between the point to be predicted and the other data points in order to discover which data points are nearest formulas such as Minkowski distance. Minkowski distance formula can be found as follows:

$$\sum_{i=1}^{n} |x_i - y_i|^{(1-p)}$$

The following algorithm may be used to describe how the K-NN works:

- Decide on the neighbors' K-numbers. Calculate the distance between K neighbors in step two.
- Based on the determined Euclidean distance, select the K closest neighbors.
- Count the number of data points in each category among these k neighbors.
- Assign the fresh data points to the category where the neighbor count is highest.
- Our model is complete.

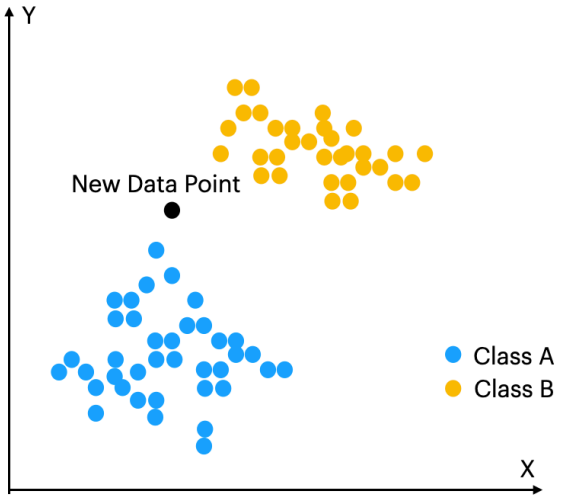

Figure 2.4: KNN Illustration

2.2.7 Support Vector Machine (SVM)

A support Vector Machine is a model used to solve problems with classification and regression. It works well for many real-world issues and can solve both linear and non-linear problems. The SVM concept is straightforward: A line or a hyperplane that divides the data between classes is produced by the algorithm.

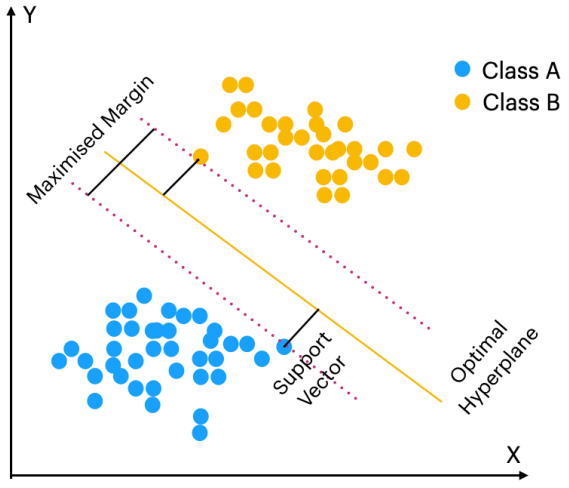

Figure 2.5: SVM Illustration

Moreover, SVM attempts to fit a hyperplane that optimally separates the data points after mapping the data into higher-dimensional space using the appro-

priate Kernel function if the data is not linearly separable as shown in Figure 2.5. An SVM algorithm works by first, mapping data to a high-dimensional feature space so that data points can be categorized, even when the data are not otherwise linearly separable. Then a separator is estimated for the data. The data should be transformed in such as way that a separator could be drawn as a hyperplane. A summary of the main steps that define SVM can be listed as follows:

- Mapping data to a high-dimensional feature space.
- Finding the best-fit separator so that the SVM algorithm outputs an optimal hyperplane that categorizes new samples.

2.2.8 Logistic Regression Classifier

Finding the model that best captures the connection between the dependent and independent variables is the goal of utilizing logistic regression which is illustrated in Figure 2.6. The Sigmoid function is used in logistic regression to convert predicted values to probabilities. Any real number may be transformed into a value between 0 and 1 with this function. The Sigmoid function formula is defined as follows:

$$\sigma(z) = \frac{1}{1+e^{-z}}$$

Moreover, to measure the error rate in each iteration a cost function is used. The cost function is the difference between our projected value and the actual value. The Perceptron (Rosenblatt 1958) name is also used for this method. It has been understood that the neurons can learn from and process training set items one at a time thanks to the perceptron algorithm. Every input value and its associated weights are first multiplied by the perceptron model before being added to get the weighted total. To get the desired result, this weighted sum is also applied to the activation function.

2.2.9 Evaluation Metrics for the Models

The model's performance evaluation metrics can be listed as follows: Accuracy, Precision, Recall, F1-Score, Sensitivity, and Specificity. The term accuracy refers to how many times the trained model was right overall throughout testing.

The Precision measure attempts to answer the issue of how many positive identifications were genuinely correct while the Recall measure attempts to answer what proportion of genuine positives were accurately identified. Moreover, the harmonic mean of accuracy and recall is used to get the F1-Score. Lastly, we can define the sensitivity (true positive rate) as the likelihood of a positive test result if the individual is actually positive and specificity as the likelihood of a negative test result, assuming the subject is actually negative.

We can define the formulas in terms of true positive(TP), true negative(TN), false positive(FP), false negative(FN) as follows:

$$Accuracy = \frac{TP + TN}{TP + TN + FP + FN}$$

$$Precision = \frac{TP}{TP + FP}$$

$$Recall = \frac{TP}{TP + FN}$$

$$F1 = \frac{2 * Precision * Recall}{Precision + Recall} = \frac{2 * TP}{2 * TP + FP + FN}$$

$$Sensitivity = Recall = \frac{TP}{TP + FN}$$

$$Specificity = \frac{TN}{FP + TN}$$

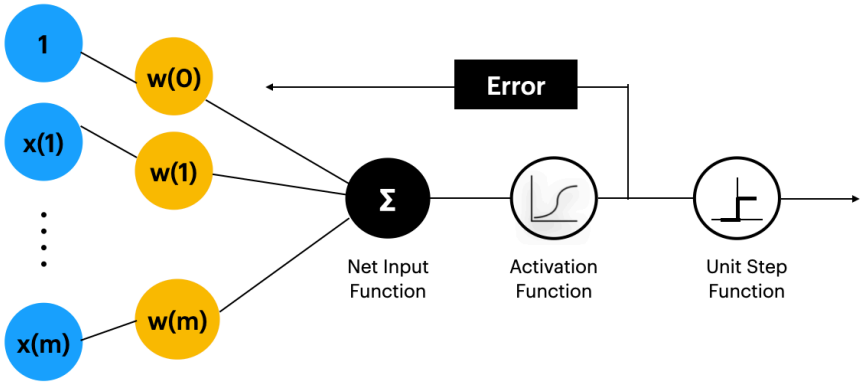

Figure 2.6: Logistic Regression Classifier Illustration

2.2.10 LIME

LIME (Local Interpretable Model Agnostic Explanations)(Ribeiro, Singh, and Guestrin 2016) is an XAI method that helps to shed light on black box artificial intelligence models in order to understand which properties are the most salient features to make the current decision.

Additionally, it builds the explanations by supplying the black-box model with minor variations of the original data point and observing how the model's predictions alter. It tries to learn an interpretable model from these different variants that estimate the black-box classifier model in the proximity of the original data point. The model g that minimizes loss L, which gauges how closely the explanation resembles the original model f's forecast, is the explanation model for example x.

$$explanation(x) = argmin_{g \in G} L(f, g, \pi_x) + \omega(g)$$

The basic steps describing how the LIME algorithm learns an explainable linear model can be listed as follows:

- Selecting the example to be described
- Modifying the sample to produce several more samples surrounding the initial one
- Using the black-box model to label the affected data.
- LIME weights the samples based on how close they are to the chosen sample in order to learn the explainable model.

An explainable linear model with sparse features, like the one learned by LIME, has this property by nature. It is possible to examine the model's weights and use them as a proxy for feature significance. As a result, the feature scores that LIME delivers are really the weights of the linear model. Figure 2.7 illustrates the whole process of explainability which utilizes LIME.

2.2.11 SHAP

A game theoretic method known as SHAP (Shapley Additive Explanations) (Lundberg and Lee 2017) is also used to explain the results of any machine learning model. Every feature is given a relevance value by SHAP for a specific prediction. Moreover, it can be described as a system for allocating compensation

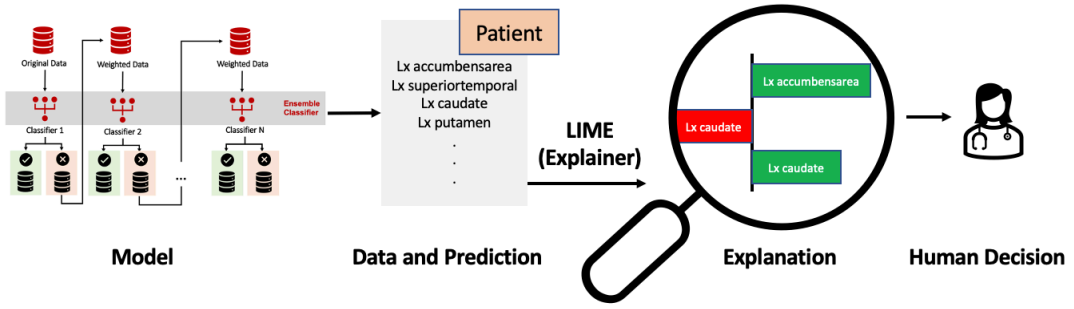

Figure 2.7: LIME implementation

to participants based on how much of the overall payoff they contributed. Players form a coalition and benefit financially from their collaboration. Ultimately, the Shapley value is the average marginal contribution of a feature value overall potential coalitions.

The many Shapley values required for the global model interpretations may be computed quickly. The approaches for global interpretation include clustering, summary plots, interactions, feature dependency, and feature significance.

The explanatory model for additive feature attribution techniques is a linear function of binary variables that can be defined as follows:

$$f(z) = g(z^{'}) = \phi_0 + \sigma_{i=1}^{M} \phi_i z_i^{'}$$

where M is the total amount of input features, $z^{'} \in \{0,1\}^M$, f(x) is the existing model, and g(x) is an ML model that was developed as a simpler explanation model. In the face of multicollinearity, Shapley regression values are feature importance for linear models.

Retraining the model using all feature subsets $S \subset F$, where F is the set of all features, is necessary for this strategy. The SHAP values show how much features influence prediction. By computing each feature's SHAP values, it is possible to verify the impact of each feature on the result.

$$\phi_i = \sum_{S \subset F \setminus \{i\}} \frac{|S|!(|F| - |S| - 1)!}{|F|!} [f_{S \cup \{i\}}(x_{S \cup \{i\}}) - f_S(x_S)]$$

S is a subset of F which is the set of all features. A model $f_{S \cup \{i\}}$ is trained with the feature present, and a model f_S is trained with the feature hidden to calculate this effect with input x_S.

2.2.12 Partial Dependence Plot (PDP)

Global explainability approaches are particularly helpful when the modeler wishes to comprehend the broad mechanisms in the data since they represent the typical behavior of a machine learning model. A partial dependency plot (Goldstein et al. 2015) can demonstrate if a goal and a feature have a linear, monotonic, or more complicated relationship. As we indicated in the materials and methods section, the fundamental justification for this is that a flat PDP implies that a feature is not significant, but a feature with a more variable PDP is more crucial. We computed PDP on the best-performing model and extracted the ROIs which do not have a flat resulting partial dependence.

2.2.13 The XGBoost Built-In Explainability Package

The XGBoost model is already explainable by design due to its decision-tree-based structure. The built-in package (T. Chen and Guestrin 2016a) has 3 different kinds of measures for the importance study. By calculating the relative contributions of each feature to each decision tree in the whole model, the type of 'gain' denotes the proportional contribution of the associated feature to the model. Moreover, the proportional number of observations connected to this feature refers to the importance type of 'coverage'. Lastly, the type of 'weight' is a proportion that indicates how frequently a specific feature appears in the model's decision trees.

3 Results

This chapter describes the level and organization of brain dopamine lateralization in healthy controls by identifying the ROIs that have significantly different distributions between the left and right hemispheres when age and gender are taken into account. Thereafter, the differences between healthy controls and patients are presented in terms of dopamine lateralization. Finally, the metrics belonging to artificial intelligence models and explainability outcomes are listed. In summary, at the end of this chapter, we'll be able to answer to following questions:

- How is lateralization of the human brain organized in Healthy Controls?
- Which are the most salient ROIs that show significant differences between the left and right hemispheres?
- How does the normal lateralization of the human brain change with age and gender factors?
- How does the lateralization change between healthy controls and patients?

3.1 Brain Dopamine Lateralization and Hemispheric Differences in Healthy Controls

First, to investigate how the Ki values change in the left and right hemispheres, we visualized the Ki values belonging to each ROI. We can observe

in Figure 3.1 that the Pallidum has the greatest mean difference (Δ = 0.001402). We can also observe that the dopamine is rightwards lateralized in the Pallidum. Moreover, the Accumbensarea (Δ=0.001401) is the second most lateralized ROI after Pallidum and is also rightwards lateralized. Further, we found that the Insula is in third place concerning the magnitude of difference (Δ=0.000455) in Ki values between right and left and it is leftwards lateralized in healthy controls. In addition, the medial orbitofrontal has a standout difference between the two hemispheres (Δ=0.000329) and it is leftwards lateralized. Considering the top five ROIs that are significantly lateralized in healthy controls, the Caudate has the fifth place and is rightwards lateralized (Δ=0.000283).

3.1.1 Wilcoxon Signed-Rank Test Between Left and Right Ki Values

We used the Wilcoxon signed-rank test, a non-parametric version of the paired t-test, to identify ROIs with notable distributional differences. The left and right Ki values belonging to the cohort of healthy controls were used in the test.

With the normalization method referring to rounding negative values to 0 and leaving positive values as original, we can observe in Figure 3.1 that the most important ROI in terms of hemispheric differences has been reported to be the Accumbensarea (p=$3.85e^{-25}$). In the second place, the Pallidum is showing a significantly different distribution between the left and right hemispheres (p=$2.91e^{-24}$). Moreover, in the third place, the Medial Orbito Frontal was nominated with an importantly different distribution between the left and right hemispheres (p=$1.06e^{-23}$). Additionally, considering the hemispheric differences in dopamine Ki values distribution, in the fourth and fifth places, the Insula (p=$7.26e^{-23}$) and the Superior Temporal (p=$3.68e^{-15}$) were reported.

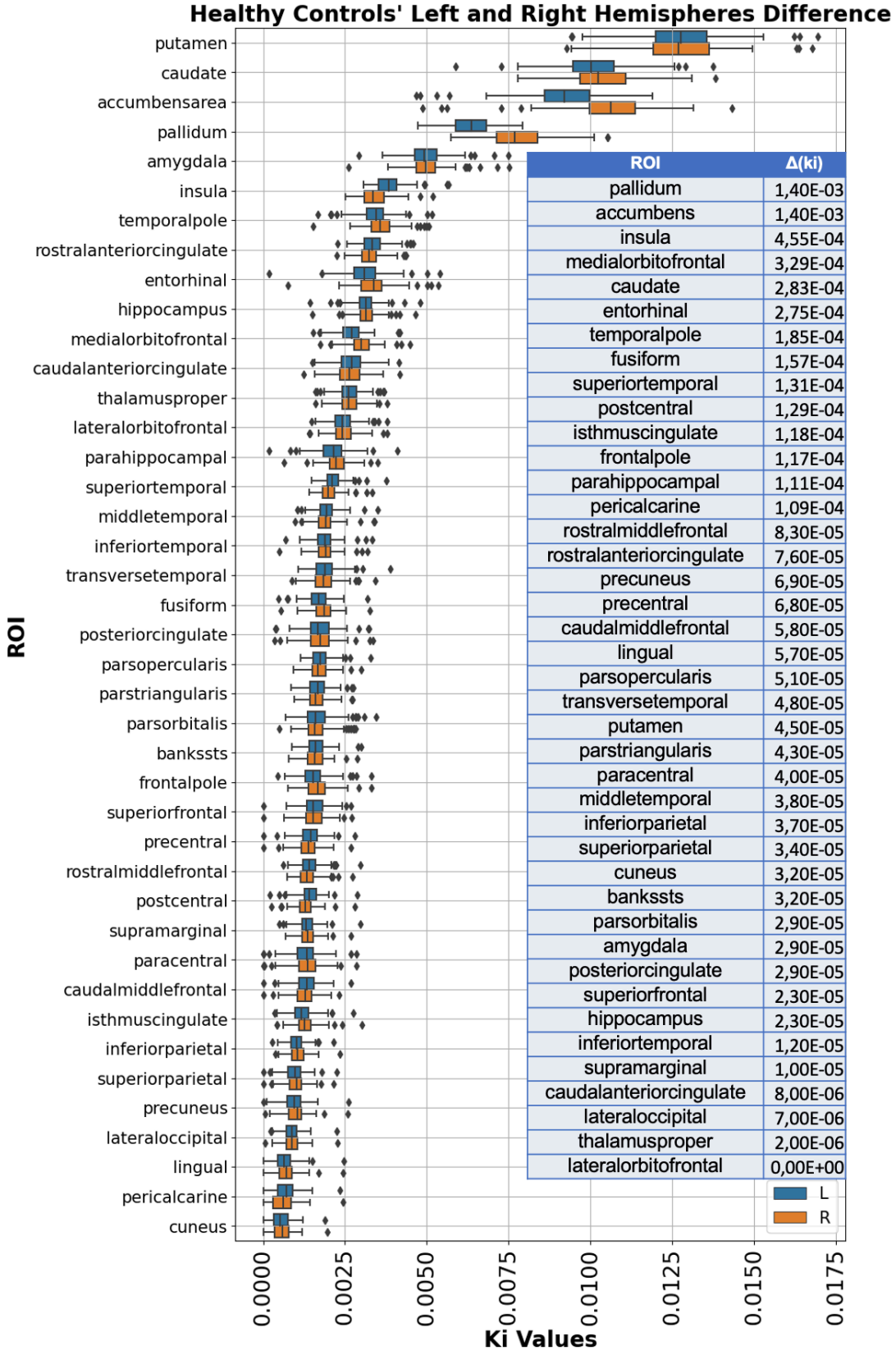

ROI	Δ(ki)
pallidum	1,40E-03
accumbens	1,40E-03
insula	4,55E-04
medialorbitofrontal	3,29E-04
caudate	2,83E-04
entorhinal	2,75E-04
temporalpole	1,85E-04
fusiform	1,57E-04
superiortemporal	1,31E-04
postcentral	1,29E-04
isthmuscingulate	1,18E-04
frontalpole	1,17E-04
parahippocampal	1,11E-04
pericalcarine	1,09E-04
rostralmiddlefrontal	8,30E-05
rostralanteriorcingulate	7,60E-05
precuneus	6,90E-05
precentral	6,80E-05
caudalmiddlefrontal	5,80E-05
lingual	5,70E-05
parsopercularis	5,10E-05
transversetemporal	4,80E-05
putamen	4,50E-05
parstriangularis	4,30E-05
paracentral	4,00E-05
middletemporal	3,80E-05
inferiorparietal	3,70E-05
superiorparietal	3,40E-05
cuneus	3,20E-05
bankssts	3,20E-05
parsorbitalis	2,90E-05
amygdala	2,90E-05
posteriorcingulate	2,90E-05
superiorfrontal	2,30E-05
hippocampus	2,30E-05
inferiortemporal	1,20E-05
supramarginal	1,00E-05
caudalanteriorcingulate	8,00E-06
lateraloccipital	7,00E-06
thalamusproper	2,00E-06
lateralorbitofrontal	0,00E+00

Figure 3.1: Left and Right Differences in Healthy Controls

Rank	ROI	Statistics
0	Accumbens	8.00
1	Pallidum	105.00
2	Medial Orbitofrontal	168.00
3	Insula	263.00
4	Superior Temporal	1245.00
5	Post Central	1247.00
6	Fusiform	1334.00
7	Rostral Middle Frontal	1527.00
8	Entorhinal	1698.00
9	Caudate	2083.00
10	Precentral	2065.00
11	Precuneus	2131.00
12	Isthmus Cingulate	2345.00
13	Pericalcarine	2770.00
14	Temporal Pole	2837.00
15	Lingual	2952.00
16	Caudal Middle Frontal	3001.00
17	Superior Parietal	3079.00
18	Inferior Parietal	3203.00
19	Frontal Pole	3269.00
20	Parahippocampal	3384.00
21	Rostral Anterior Cingulate	3477.00

Table 3.1: Healthy Controls Wilcoxon Test Results
The above table illustrates the results belonging to healthy controls data normalized according to the approach of rounding negative values to 0 and leaving positive values as original. All above-listed ROIs had p-values smaller than p=0.00125 (Bonferroni Corrected). The statistics column indicates the sum of the ranks of the differences.

3.1.2 Non-Parametric ANCOVA Test (Quades' Method) - Lateralization Differences of ROIs Among Healthy Controls

The first experiment has been designed among only a healthy control group while taking age as a covariate and gender as a factor considering the calculated lateralization indices as dependent values.

In this section, first, we calculated the lateralization indices belonging to each 81 bilateral regions. Thereafter to understand in which regions the dopamine lateralization is significantly different in men and females taking the age factor

into consideration. There are two regions became prominent with p-values less than 0.05 threshold as a result of this experiment. These regions are listed as the Inferior Parietal (p = 0.039) and the Transverse Temporal (p = 0.004). Therefore, we can observe that in these regions men and female individuals in healthy cohorts have significantly different dopamine lateralization.

ROI	**t**	**p-value**
Inferior parietal	-2.089	0.039
Transverse temporal	-2.892	0.004

Table 3.2: Healthy Controls Quades' Test Results
The normalization approach here references rounding negative values to 0 and leaving positive ones as original. Following the calculation of lateralization indices, these indices have been normalized between -1 and 1.

3.1.3 Age and Gender Factors Effect to Lateralisation Changes in Healthy Controls

ROI	**Gender**	**r**	**p-value**	**Lx**
Thalamus	Female	0.46	0.00024	←
Postcentral	Female	0.44	0.00041	←
Cuneus	Female	-0.40	0.0015	→
Bankssts	Female	0.37	0.004	←
Caudalmiddlefrontal	Male	-0.30	0.0055	→
Precuneus	Female	-0.35	0.0062	→
Putamen	Female	-0.34	0.0079	→
Superiorparietal	Female	0.30	0.021	←
Parstriangularis	Male	-0.25	0.022	→
Medial orbitofrontal	Male	-0.24	0.027	→
Isthmus cingulate	Male	-0.24	0.027	→
Precentral	Female	0.27	0.036	←
Temporalpole	Male	0.23	0.039	←
Temporalpole	Female	0.26	0.041	←
Parstriangularis	Female	-0.26	0.045	→

Table 3.3: Lateralization bias change with age
Significant ROIs of the DK atlas resulting from regression analysis in Hcs. The ← indicates that the healthy controls ROI is left-lateralized with age and the → indicates that the healthy controls ROI is right-lateralized with age.

According to Table 4.3 results of healthy controls linear regression, we detected a significant effect of age on the lateralization of some ROIs. The Thalamus which is illustrated in Figure 3.2 was reported as the most significant region which is left-lateralized depending on the aging factor in the female cohort. Meaning that, as the age of female increase, dopamine is more lateralized to the left hemisphere.

Another significant ROI that has been frequently involved in dopamine research and produced significant results in terms of lateralization depending on age is Putamen. As the age of the healthy female cohort increase, the dopamine lateralization index value of Putamen increases (it tends to be more rightwards lateralized). However, we have not observed a such significant change in the healthy male cohort as can be also observed in Figure 3.3.

When we further investigate the ROIs that were affected by the age and gender factors in terms of lateralization differences, in the second place Post Central was prominent as visualized in Figure 3.4. The dopamine lateralization in Post Central increases significantly in parallel with age in the female cohort. Even though the male cohort shows adverse effects, it is not significantly associated with age.

Moreover, in Cuneus there is a significant drop in lateralization index value with the increasing age considering the female cohort (it tends to be more rightwards lateralized). However, as visualized in Figure 3.5 the lateralization index follows a more flat trend considering the aging factor in the male cohort.

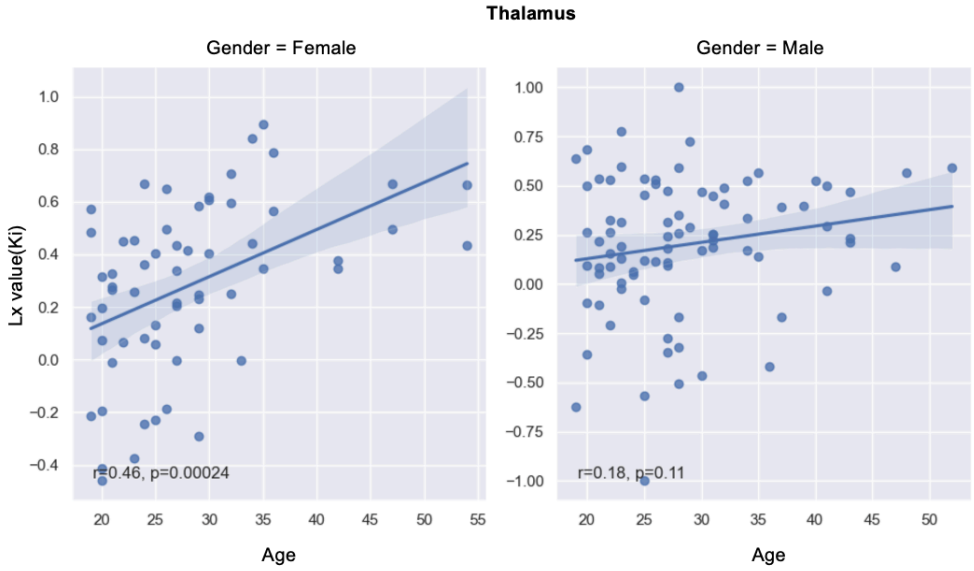

Figure 3.2: Thalamus Lateralization Depending on the Age and Gender Factors
The above figure illustrates how the Thalamus is lateralized depending on age and gender factors. In the female cohort, as the individual age, dopamine is tended to be left-lateralized (p=0.00024) even though in the male cohort no significant change depending on age has not been observed (p=0.11).

Figure 3.3: Putamen Lateralization Depending on the Age and Gender Factors
The above figure illustrates how the Putamen is lateralized depending on age and gender factors. In the female cohort, as the individual age, dopamine is tended to be right-lateralized (p=0.0079) even though in the male cohort no significant change depending on age has not been observed (p=0.079).

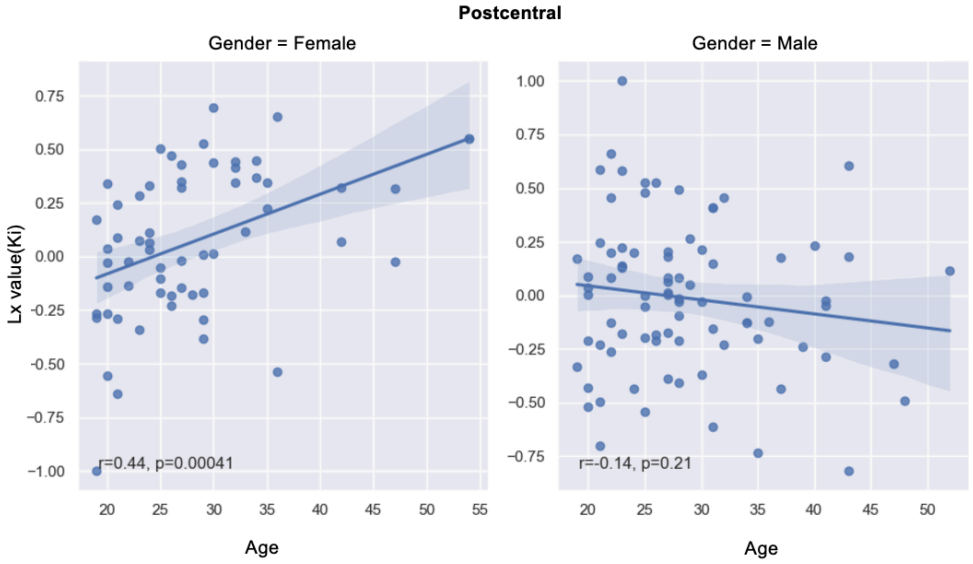

Figure 3.4: Post Central Lateralization Depending on the Age and Gender Factors

The above figure illustrates how the Post Central is lateralized depending on age and gender factors. In the female cohort, as the individual age, dopamine is tended to be left-lateralized (p=0.00041) even though in the male cohort no significant change depending on age has not been observed (p=0.21).

Figure 3.5: Cuneus Lateralization Depending on the Age and Gender Factors

The above figure illustrates how the Thalamus is lateralized depending on age and gender factors. In the female cohort, as the individual age, dopamine is tended to be right-lateralized (p=0.0015) even though in the male cohort no significant change depending on age has not been observed (p=0.83).

3.2 Dopamine Lateralization of Patients' Brain and Differences with Healthy Controls

We will discuss the differences in dopamine lateralization between cohorts of healthy controls and patients in this chapter. The ROIs with the largest gaps when compared to healthy controls can provide information about possible future treatments and medications. At the end of this chapter, we will be able to answer the following questions:

- Which ROIs lead to the difference between healthy controls and patients?
- Which are the ROIs a decision-making mechanism takes into consideration when differentiating between healthy control and a patient?

3.2.1 Non-parametric ANCOVA Test (Quades' Method) - Lateralization Differences of ROIs Between Healthy Controls and Patients

Non-parametric ANCOVA was used in this section, with cohorts acting as a grouping factor, age and gender as covariates, and the dependent variable serving as the lateralization index. According to Table 4.4. Accumbens ($p < 0.01$) is showing the most significant difference in dopamine lateralization when comparing healthy controls and patients. In the second place, we observe that Putamen ($p < 0.01$) is also playing a key role to differentiate between the two cohorts. Moreover, we also found out that Supramarginal ($p < 0.05$), Caudal Anterior Cingulate ($p < 0.05$), and Pallidum ($p = 0.05$) can be focal ROIs to investigate differences between healthy controls and patients.

Moreover, we grouped the same ROIs and calculated the mean values. Thereafter, to demonstrate the differences between healthy and patient cohorts in terms of lateralization indices, we calculated the differences with absolute values. We can observe in Figure 3.6 that the top 5 ROIs which have the greatest gaps are as follows: the Accumbens (Δ=0.108), the Putamen (Δ=0.095), the Cuneus (Δ=0.069), the Frontal Pole (Δ=0.069), and the Caudal Anterior Cingulate (Δ=0.064). We can also observe that considering Accumbens, dopamine lateralization in healthy controls and patients has the same direction (rightwards) but it is more lateralized in healthy controls. Similarly, in Putamen both cohorts

ROI	**t**	**p-value**
Accumbens	-3.708	0.000
Putamen	3.768	0.000
Supramarginal	-2.158	0.032
Caudal Anterior Cingulate	2.096	0.037
Pallidum	-1.954	0.052

Table 3.4: Healthy Controls vs Patients Quades' Test Results
The normalization approach here references rounding negative values to 0 and leaving positive ones as original. Following the calculation of lateralization indices, these indices have been normalized between -1 and 1.

follow the same lateralization direction (leftwards) but Putamen is more lateralized in Healthy controls.

Further, to demonstrate all ROIs visually on the brain, we utilized the Brain Painter (R. V. Marinescu et al. 2019) tool by MIT to visually outline the lateralization value differences between healthy controls and patients referencing the ROIs based on DK Atlas as illustrated in Figure 3.7. Lateralization index differences belonging to each ROI have been calculated by rescaling the Ki values between 0-5, then differencing the two cohorts of healthy controls and patients, and finally rescaling the results again between 0-5.

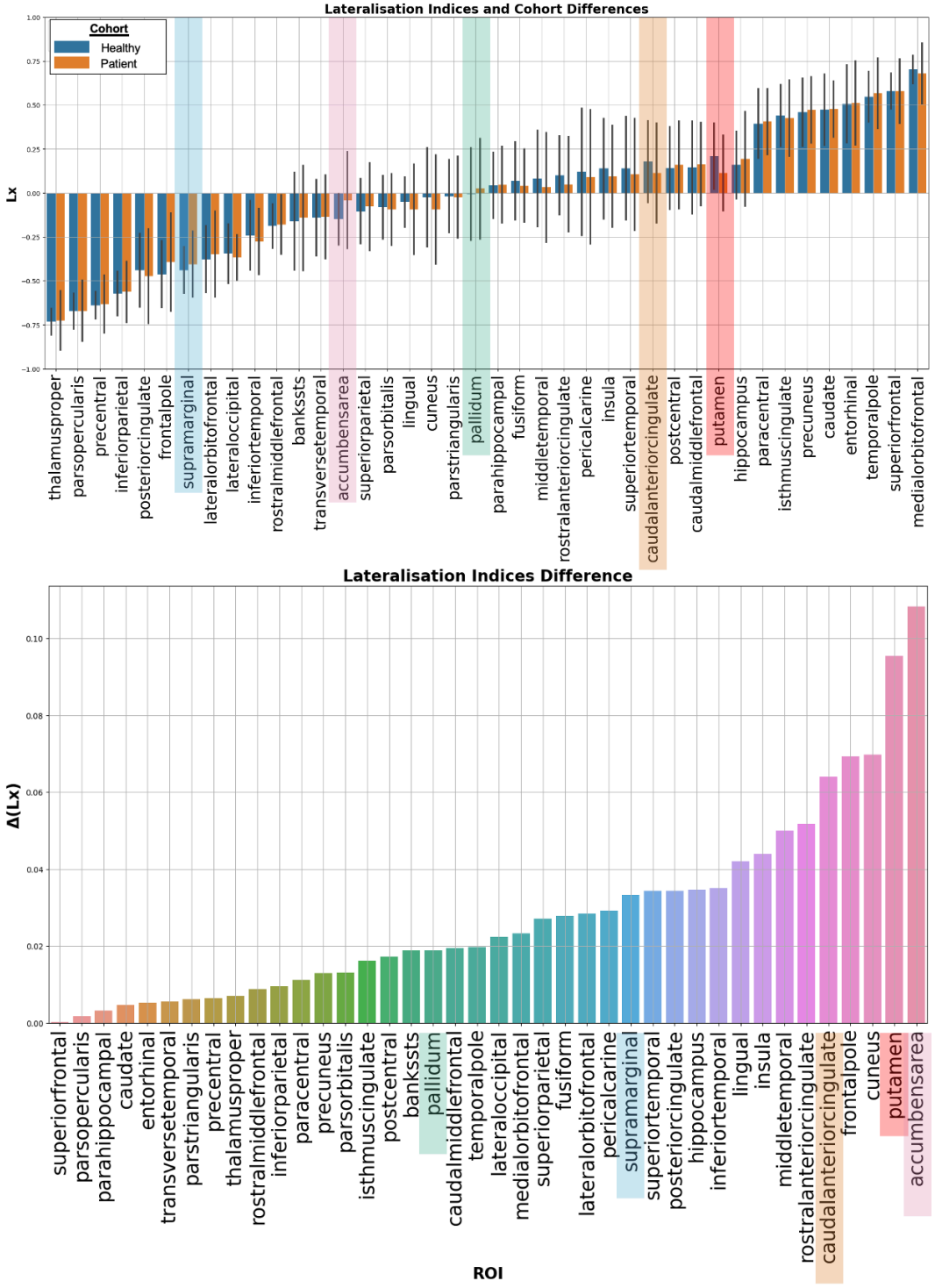

Figure 3.6: Difference Distribution of Lateralization Indices
The above figure illustrates the results belonging to lateralization indices difference between healthy controls and patients data. Lateralization indices are normalized between -1 and 1. Thereafter the ROIs are grouped and mean difference values are calculated.

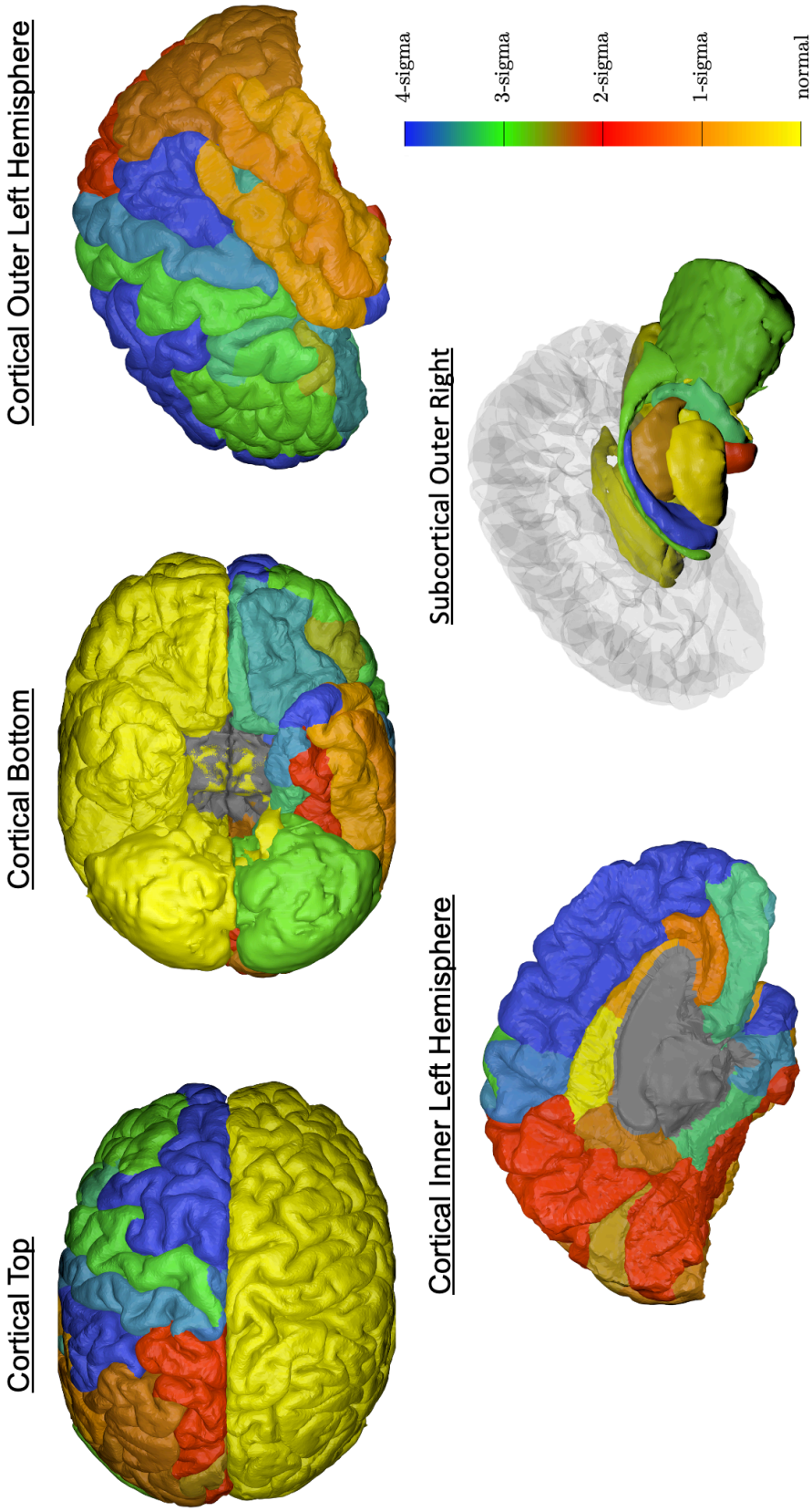

Figure 3.7: Brain Painter
The cortical top, cortical bottom, cortical outer left hemisphere, cortical inner left hemisphere, and subcortical outer right angles have been visualized. See the appendices for the DK atlas ROI labels.

3.2.2 Classifier Models Performance

The next stage is to use a classifier to evaluate the findings of our statistical analysis in order to use artificial intelligence to discover underlying patterns in a data-driven way. We tested various models to determine which one performed the best, and we used the post hoc model agnostic explainability method LIME to identify the most important regions that influenced the model's choice. Moreover, to determine which regions have the greatest influence on the classifier's conclusion, the models were given lateralization indices data from both patients and healthy controls without age or gender information.

The optimization parameters that have been used for hyper-parameter optimization details can be found in the following Table 4.5.

ROI	**Parameters**
XGBoost Classifier	learning rate = 0.1 colsample bytree=0.9 colsample bylevel= 0.9 colsample bynode=0.9 max depth = 16 n estimators = 1000
Random Forest Classifier	max depth=2 random state=0
KNN	n neighbours = 5
SVM	c=1 kernel='rbf' degree=3

Table 3.5: Models Hyper-Parameter Setting and Organization

After the training phase, the models have been tested with a test set that was reserved initially as 25% of the whole dataset and unseen during the training. As a result, even though the XGboost and Random Forest Classifiers ended up with the same accuracy of 76% XGBoost Classifier had greater precision of 79% and specificity of 79%.

ROI	Accuracy	Precision	Recall	F1-Score	Sensitivity	Specificity
XGBoost Classifier	0.79	0.79	0.79	0.78	0.79	0.78
Random Forest Classifier	0.71	0.82	0.71	0.69	0.71	0.71
Logistic Regression	0.57	0.77	0.57	0.71	0.57	0.57
Naive Bayes	0.79	0.85	0.79	0.78	0.78	0.78
SVM	0.50	0.25	0.50	0.33	0.50	0.50
KNN	0.71	0.71	0.71	0.71	0.71	0.71

Table 3.6: Trained Model Metrics Results
The training data is 75%, and the test set is 25% of the whole dataset. The training data has been shuffled before feeding into the model.

Further, we investigated the confusion matrix and Receiver Operator Characteristic ROC curve regarding the best-performing model of the XGBoost Classifier. We can observe that the model is good at diagnosing actual patients regarding the 41.18% rate of True Positive and struggling to distinguish actual healthy controls regarding the 17.65 % rate of False Positive.

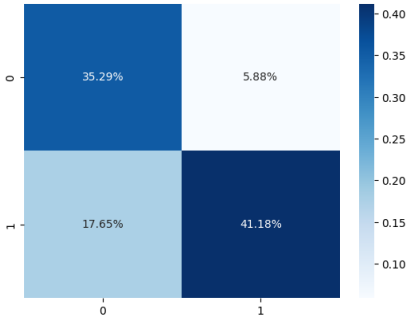

Figure 3.8: Confusion Matrix - XGBoost Model
The above figure illustrates the results belonging to the XGBoost Classifier model. The healthy cohort is encoded as 0, and the patient cohort is encoded as 1. The True Positive rate is 41.18%, the False Negative rate is 5.88%, the False Positive rate is %17.65, and the True Negative rate is reported as 35.29%. The horizontal values are actual values, and the vertical values are predicted values.

3.2.3 Global Explainability - Partial Dependence Plots(PDP)

Having concluded that the Putamen is highly lateralized in healthy controls with statistical analysis results, in this section PDP is also verifying that when the lateralization of dopamine in the Putamen increases, the probability of being diagnosed with Schizophrenia decreases. Moreover, when the Pallidum lateralization index exceeds the 0 threshold and increases, the probability of being diagnosed with Schizophrenia increases. The Accumbens is also following a similar pattern to Pallidum however it has a lower threshold (t=-0.2). Additionally, we can observe that when the lateralization index belonging to Posterior Cingulate is lower than the threshold (t=-0.2), the probability of being diagnosed is high. Another significant change can be observed when the lateralization index of Fusiform exceeds the threshold value of 0. When the Fusiform lateralization index value exceeds 0, in other words when the lateralization is more left-wards, the probability of being diagnosed with Schizophrenia decreases and the person becomes healthier. Figure 3.9 lists the ROIs with stood-out variance in predicted probabilities and other ROIs fitted to flatter dependence plots.

3.2.4 XGBoost Built-In Explainability

According to the built-in analysis as illustrated in Figure 3.10, using the importance type of 'gain', the Insula (w = 0.163) is the brain region with the highest differential dopamine lateralization between controls and patients, and the most relevant feature for the classification. Moreover, the Cuneus (w=0.161), Hippocampus (w=0.155), Precuneus(w=0.141), and Parahippocampal (w=0.041) were reported in the list of the top 5 most significant regions with the importance type of 'gain' with XGBoost Classifier built-in importance function. On the other hand, with the importance type of 'weight', the leading ROI is the Precuneus (w= 8.0) and Insula (w=0.8). The Hippocampus (w=3.0), Parahippocampal (w=1.0), and Cuneus (w=1.0) were reported in the top 5 significant regions additionally. Finally, the important type of 'cover' has outlined the Hippocampus(w=2.7), the Precuneus (w=2.3), the Insula (w=2.2), the Cuneus (w=2.1), and the Parahippocampal (w=2.00) in the top 5 ROIs that affects the decision made by the XGBoost classifier model.

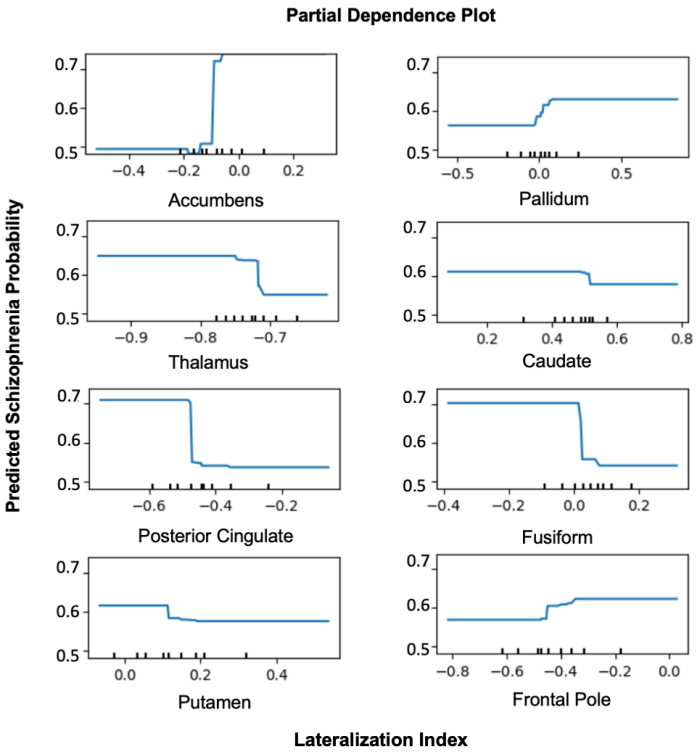

Figure 3.9: Partial Dependence Plot - XGBoost Model
Partial Dependence Plot of Prediction Probability of Being Diagnosed with Schizophrenia. Healthy controls are as encoded 0 and patients are encoded as 1. The x-axis shows the lateralization indices data specific to that region and the y-axis shows the prediction probability of being diagnosed with psychosis.

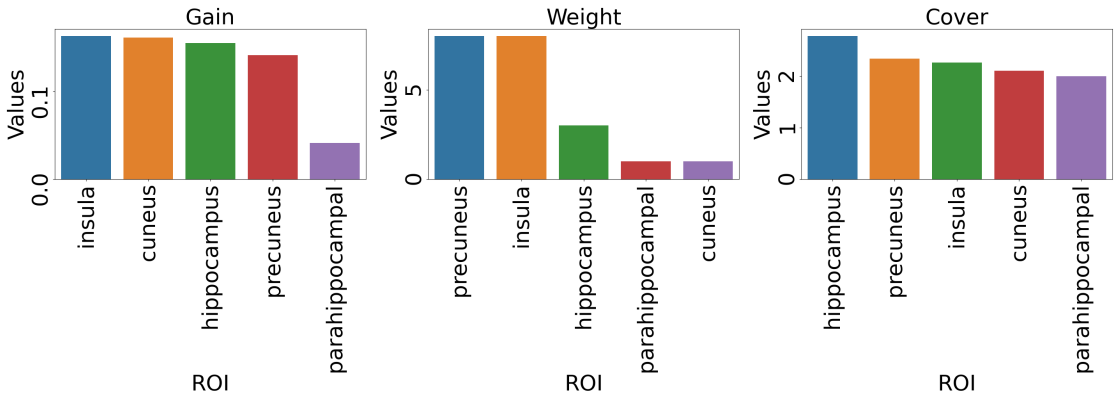

Figure 3.10: Partial Dependence Plot - XGBoost Model
The above figure illustrates the results belonging to the XGBoost Classifier model. The classes have been encoded as follows: 0 is healthy control and 1 is patient.

3.2.5 Local Explainability - LIME

We applied the LIME method which is explained in detail in the section of analysis due to its model-agnostic offer in terms of applicability. To investigate in detail which ROIs are nominated by the XGBoost Classifier during the classification task of differentiating between healthy controls and patients with psychotic symptoms, we will report further precise sample-based explanations.

Looking at the explanations produced by the LIME, we can conclude for a specific patient that the Accumbens, Putamen, and Pallidum increased the chance of being diagnosed with Schizophrenia. On the other hand, ROIs such as Posterior Cingulate, Inferior Temporal, and Frontal Pole decreased the chance of being diagnosed with Schizophrenia. This may provide a great opportunity for researchers to focus on specific areas which increased the chance of diagnosis as visualized in Figure 3.11.

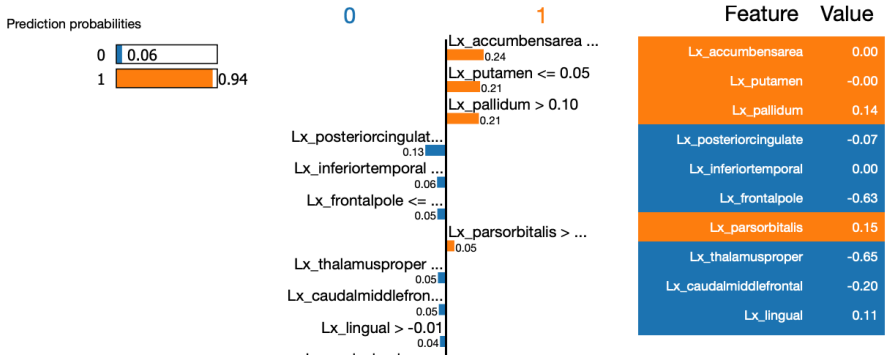

Figure 3.11: Precise Explanations - LIME
The above figure illustrates the resulting post hoc local explanations belonging to a patient. The class '0' represents patients and the class '1' represents patients. The right-hand-side table lists the thresholds belonging to the most salient features. The middle graph represents features and their individual contributions to the voting scheme for the decision to be made by the model.

3.2.6 Shapley Additive Explanations - SHAP

Instead of producing sample-based local explanations as in the case of LIME, to further investigate the general behavior of the model regarding the task of differentiating between healthy controls and patients, we produced the feature significance weights with the SHAP method. According to the results, the Accumbens (w=1.11) is the most significant region that can be used to differentiate between healthy controls and patients. The Fusiform (w=0.89), Posterior

Cingulate (w=0.85), Thalamus Proper(w=0.64), Pallidum (w=0.5), Pericalcarine (w=0.42), Frontal Pole(w=0.41), Putamen (w=0.4), and Caudate (w=0.25) have been reported as significant in the top 10 ROIs.

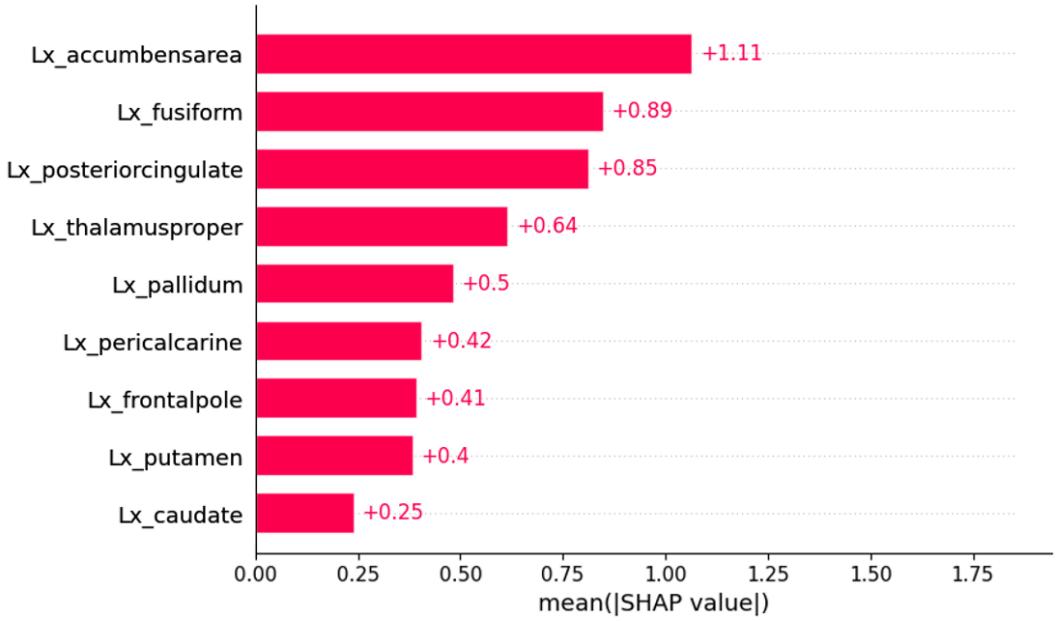

Figure 3.12: SHAP Explanations
The above figure illustrates the resulting post hoc explanations explaining the overall behavior of the model. The top 10 most significant ROIs have been outlined.

Thus, when the classifier model tries to make a classification between healthy controls and patients, it puts more emphasis on the sorted list of ROIs as illustrated in Figure 3.12. Therefore, a clinician may refer to that kind of decision-support tool to see which ROIs on the brain may be a strong indicator of possible findings which may be helpful in decision-making.

4

Discussion and Conclusions

In this research study, our comprehensive data analysis showed that human brain dopamine is lateralized in a specific organization on healthy controls and there is a visible difference in lateralization between healthy controls and patients by investigating healthy controls data from 142 Healthy Controls (HC, age: 28.3±7.7 yrs [$\mu \pm \sigma$, range: 19-54]) and Schizophrenia patients with psychotic symptoms with the addition of 136 patients' data (age: 32.0±10.7 yrs [$\mu \pm \sigma$, range: 18-65]) through $[^{18}F]FDOPA$ imaging method. Regarding the dopamine lateralization of healthy controls, we observed the greatest mean absolute difference in the following top 5 ROIs: Pallidum (Δ=0.0001402, $R_{Ki} > L_{Ki}$), Accumbensarea (Δ=0.001401, $R_{Ki} > L_{Ki}$), Insula (Δ=0.000455, $L_{Ki} > R_{Ki}$), Medial Orbital Frontal (Δ=0.000329, $L_{Ki} > R_{Ki}$), and the Caudate (Δ=0.000283, $R_{Ki} > L_{Ki}$). Additionally, we applied the Wilcoxon signed-rank test between left and right Ki values to understand which ROIs have significantly different distributions. As a result of the Wilcoxon test, Accumbens (p=0.0), Pallidum (p=0.0), Medial Orbital Frontal (p=0.0), Insula (p=0.0), and Superior Temporal (p=0.0) were nominated to have significantly different distributions in both hemispheres.

However, to observe if lateralization change is highly associated with age and gender factors, we applied simple linear regression to the lateralization indices belonging to the most salient ROIs, to investigate further age and gender effects. We observed that in the female cohort, ROIs such as the Thalamus(p=0.00024), Postcentral (p=0.00041), Cuneus (p=0.0015), Putamen (p=0.0079), and in the male cohort, ROIs such as Caudal Middle Frontal (p=0.0055), Parstriangularis (p=0.022), Isthmus of Cingulate(p=0.027), Temporal Pole (0.041) lateralization change is

highly dependent on aging. For instance, regarding Thalamus, in the female cohort, along with the increasing age, dopamine tended to be left-lateralized (p=0.00024) even though in the male cohort shows no significant change dependent on age has not been observed (p=0.11). Considering another ROI, Putamen, in the female cohort, as the individual aged, dopamine tended to be right-lateralized (p=0.0079) even though in the male cohort shows no significant change dependent on age has not been observed (p=0.079).

Therefore, we concluded that some ROIs' dominant hemisphere in dopamine lateralization and magnitude of Ki level change with increasing age in healthy controls. Moreover, the healthy state of lateralization is not only highly dependent on aging but also dependent on gender according to linear regression results. Further to investigate the gender factor by taking the age factor into consideration, we applied Quades' Test (Non-Parametric - ANCOVA). Applying the Quades' Test, gender as a grouping factor, and age as a covariate, the Inferior Parietal (p=0.039) and Transverse Temporal (p=0.004) have been reported to have significantly different lateralization organization in healthy controls.

Having concluded the results above, dopamine lateralization in the brain undergoes significant alterations with aging that have an impact on cognitive functions. Additionally, it has been reported by several clinical evidence that the dopamine system in the brain shows notable decreases with healthy aging, and these declines have been associated with impaired cognition (Y. Wang et al. 1998; Bäckman et al. 2000; Mozley et al. 2001; Erixon-Lindroth et al. 2005). Individual variations in dopamine have a significant impact on executive functions, particularly cognitive agility, even among healthy young individuals (Cools et al. 2008; Stelzel et al. 2010; Samanez-Larkin et al. 2013). Hence, dopamine represents a key target for research into the neurochemical foundations of diversity in brain lateralization in the population and may be a key factor in aging-related alterations.

Regarding the Inferior Parietal Lobule (IPL)'s significantly different lateralization between different genders according to our research, there has been no specific evidence in the literature however, some clinical research verified that the right IPL was noted as a crucial area for visuospatial attention in systematic evaluations and it was generally agreed that language function lateralizes to the (dominant) left hemisphere, in opposition to visuospatial attention (Friederici 2017). Basic attention to linguistic and social cognition, which define human relationships, are all underpinned by the inferior parietal lobe (IPL), a crucial neu-

rological substrate (Numssen, Bzdok, and Hartwigsen 2021). Moreover considering the association with Schizophrenia, the frontal-limbic-temporal-parietal neural network implicated in the Schizophrenia illness process appears to include the inferior parietal as an essential but largely unappreciated component. Compared to the prefrontal cortex, hippocampus, or cingulate, the parietal cortex, and the IPL in particular, have gotten comparatively little study, despite the fact that it is generally accepted that they play a significant role in Schizophrenia network dysfunction (Torrey 2007).

Considering Transverse Temporal which is the second ROI that is significantly distributed in men and women (p=0.004), there have been several research in the literature. The region which is known as Brodmann area 42 (Ardila, Bernal, and Rosselli 2016) is made up of the auditory cortex and transverse temporal gyri. The auditory cortex, often referred to as the posterior transverse temporal area (Elston and Garey 2013), is a region of the cerebral cortex that is situated superiorly within the temporal lobe. It is a functional area that has been discovered to have a crucial role in hearing. The sensory perception of hearing sounds with no external trigger is known as an auditory hallucination. Despite not being unique to schizophrenia, this symptom is notably linked to it and other psychotic diseases. More than 70% of people with Schizophrenia experience auditory hallucinations, making it one of the most prevalent symptoms. Additionally, according to a study, auditory hallucinations are lateralized to left temporal lobe-generated speech perceptions (Hugdahl et al. 2008).

Further, our research revealed lateralization in some ROIs is more prominent among others considering the difference between the left and right hemispheres in terms of Ki levels. Regarding this Medial Orbital Frontal was nominated to sustain higher Ki levels of dopamine in the left hemisphere than the right hemisphere. Moreover, human neuroimaging studies have validated the orbital frontal cortex's function as a hub for sensory integration, control of the visceral response, and involvement in learning, forecasting, and decision-making for emotional and rewarding behaviors (Kringelbach 2005). Since then, more research has supported the medial orbitofrontal cortex's function in seeing and understanding the reward potential of inputs without immediate behavioral repercussions. Additionally, research results also showed that it could work as a general outcome monitoring system, separate from tangible reward (Schnider, Treyer, and Buck 2005).

Prior research studies report that the Thalamus is an area of particular con-

cern in Schizophrenia (A. F. Oke and Adams 1987; Rao et al. 2010; Jiang, Patton, and Zakharenko 2021; Perez-Rando et al. 2022; Harms et al. 2007; Pergola et al. 2015; Pergola et al. 2015). It is intricately related to the cortex and essential for coordinating signaling to and within cortical regions (Hwang et al. 2017; Wagner et al. 2015). Moreover, one previous research reported that patients with Schizophrenia have higher levels of dopamine in their Thalamus (A. F. Oke and Adams 1987). Additionally, concerning lateralization research, previously it is reported that in the human thalamus, norepinephrine is distributed in a distinctly lateralized manner and Norepinephrine is abundant in the left hemisphere of the brain's pulvinar area, but it is more abundant in the right hemisphere of the brain's somatosensory input region (A. Oke et al. 1978). However, there hasn't been any specific research done on how Thalamus lateralization changes in healthy controls as we age.

Referring to our analysis results proving the lateralization difference in healthy controls and patients following ROIs showed significant dopamine lateralization: the Accumbens(d=0.108265), the Putamen(d=0.095546), the Cuneus (d=0.069798), the Frontal Pole(d=0.069316), and the Caudal Anterior Cingulate(d=0.064009). Considering Accumbens, dopamine lateralization in healthy controls and patients have the same direction (rightwards) but it is more lateralized in healthy controls. Similarly, in Putamen both cohorts follow the same lateralization direction (leftwards) but Putamen is more lateralized in Healthy controls. Therefore, we conclude that both the magnitude of Ki and the direction of lateralization bias differ between healthy controls and patients. Further with Quades' Non-Parametric ANCOVA by taking age and gender as covariates, our research outlined the following regions: Accumbens(p=0.000), Putamen(p=0.000), Supra Marginal(p=0.032), Caudal Anterior Cingulate(0.037), Pallidum(p=0.052). The putamen was one of the most significant ROIs considering the differentiation between healthy controls and patients in terms of dopamine lateralization. Regarding this, it has been reported that dopamine is a key neurotransmitter in the brain that is abundant in the putamen, a subcortical node located within the striatum. Additionally, the putamen is closely linked to dopamine-related psychiatric and neurodegenerative conditions that show up as motor dysfunction, impulsive behavior, and cognitive deficiencies(Luo et al. 2019). In Schizophrenia, dopamine is crucial for complex thinking and acting (Schultz 2007). The extra dopamine in the striatum (which includes the putamen) is thought to contribute to symptoms like delusions in Schizophrenia, based on the dopamine

hypothesis (Toda and Abi-Dargham 2007).

The majority of the studies examined the physical changes to the putamen, and it was shown that in healthy controls the volume of putamen decreased with aging (Dyck et al. 2002) and that there was a substantial difference between men and women (McDonald et al. 1991; Abedelahi et al. 2013). For instance, it was discovered that only among males was an age-related drop in its volume (Raz, Torres, and Acker 1995). When dopaminergic neurons in the nigrostriatal pathway are highly expressed, the dopamine-rich putamen may enlarge and result in Schizophrenia spectrum disorders (Hokama et al. 1995). Another research that experimented with whole basal ganglia reported that Schizophrenic patients displayed larger volumes when compared to healthy individuals: 14.2% for the whole basal ganglia, 27.4% for the globus pallidus, 15.9% for the putamen, and 9.5% for the caudate (Mamah et al. 2007). Concerning dopamine lateralization in the Putamen, it is only shown in one research that left-lateralized dopaminergic regulation of activity in the brain and functional networks causes lateralization of human speech (Fuertinger et al. 2018). The caudate, on the other hand, appears to have a contribution to motor planning and motor learning, despite the fact that there is strong evidence that the putamen is primarily involved in motor execution(Albin, Young, and Penney 1989). It has been suggested that motor lateralization in humans may be connected to the asymmetric nigrostriatal dopamine system which includes mainly the caudate and putamen. (de la Fuente-Fernández et al. 2000).

Thus, we can draw the conclusion that dopamine is lateralized more saliently on the ROIs responsible for motivation and reward-oriented tasks.

Similar to putamen research compromising other ROIs regarding the difference between healthy controls and people with neurodegenerative illnesses, depending on age and gender, also primarily focused on morphological changes. For instance, results of a comprehensive study revealed that in the case of Schizophrenia, there are aberrant decreases in the variability of cortical thickness in the right and left cuneus ($\Delta = 0.68$, $p = 0.002$), right postcentral gyrus ($\Delta = 0.62$, $p = 0.004$), and right pars triangularis ($\Delta = 0.61$, $p = 0.004$) (Raz, Gunning, et al. 1997). Another study that used fractional anisotropy to examine the white matter tracts in both the precentral and postcentral gyrus during the typical aging process of the brain found that the fractional anisotropy values of the two regions varied statistically throughout genders, different ages, and in each hemisphere. Furthermore, both the precentral gyrus and postcentral gyrus fractional anisotropy

values drop over time, which is a clear sign of aging (Zhou et al. 2020).

However, it is crucial to expand these physiological investigations for more inclusive research including the neurochemicals that govern brain activity. Considering our resulting significant ROIs that have been nominated to differentiate between a patient and healthy control, brain dopamine was found to be a strong contender to be a physiologically active molecule that controls the activity of some extrapyramidal areas, particularly the Substantia Nigra, Striatum, and Pallidum (Hornykiewicz 1966). Additionally, an increasing amount of research has shown that the Ventral Pallidum plays important roles in the reward of food, social attachment, drugs of abuse, financial success, and other pleasures. The Ventral Pallidum is a basal ganglia component and is positioned as the link between the midbrain circuits for motivation and reinforcement and the cortical, amygdala, and striatal circuits for cognition and action. It serves as a crucial point of convergence for the brain circuits responsible for motivation, hedonics, and reward learning (Prasad and McNally 2019). On the other hand, the ventral pallidum is also a stage of transition for various cognitive, emotional, and motor functions as well as a convergence site for limbic reward signals. The Pallidum was also nominated as a focal point for improving reward and motivation (K. S. Smith et al. 2009). Considering lateralization of dopamine, although there have been conflicting results in humans, it did appear that the left globus pallidus has more dopamine than the right (Glick, Ross, and Hough 1982; Rossor, Garrett, and Iversen 1980).

Moreover, the precise information that dopaminergic projections that innervate the nucleus accumbens encode has been the subject of a significant body of research. The dominant theories are based on the reward prediction error (RPE) hypothesis, which postulates that dopamine modifies links between rewards and predictive signals by recording perceived faults between predictions and results (Kutlu et al. 2021). Moreover, the nucleus accumbens is a component of the neuronal network that regulates reward-seeking in response to reward-predictive cues. So, for this circuit to operate normally, dopamine release in the accumbens is necessary (Nicola et al. 2005). Dopamine release and neuronal reactivity in the nucleus accumbens, which are essential for addictive behavior, are thought to be influenced by dopaminergic neuron terminals of the insula originating in the ventral tegmental area (VTA) and substantia nigra (Kalivas and Volkow 2005). Anxiety, mood, pain, cognition, danger perception, and conscious impulses are all regulated by the insular cortex (Hardy 1985; Suhara et

al. 1992;Craig 2002;Paulus and Stein 2006). Another research proves that the insula is a viable brain region to point out for addiction, according to resounding evidence (Ibrahim et al. 2019).

Additionally, many cognitive and neurocognitive investigations have been conducted on the cingulate gyrus. It has been linked to Alzheimer's disease, anxiety disorders, addiction, depression, bipolar disorder, and Schizophrenia, among other things. Regarding research focusing on structural abnormalities in adolescents, within the right cingulate cortex, scientists discovered a significant group effect in the caudal anterior cingulate (F=2.9, p=.057): with lower cortical thickness in the high-risk psychosis group compared to healthy controls. Another research experimented with 22 patients with Schizophrenia and 22 normal volunteers also reported that a lower volume of the caudal anterior cingulate gyrus was also associated with more serious evidence of Schizophrenia (Choi et al. 2005). Furthermore, the anterior cingulate has been shown to be important for several elements of instrumental behavior, such as learning and effort-based decision-making in the context of dopamine activity (Aly-Mahmoud et al. 2017).

Lastly, there were a few studies that previously included supra marginal in their research. However, a PET research using a D_1 receptor tracer to investigate the hereditary and nongenetic contributions to D_1 receptor binding in Schizophrenia found a significant age effect that leads to deterioration with age in the supramarginal gyrus (p=0.021)(Hirvonen et al. 2006). Another research examined the association between dopamine D_2 receptors in the brain and regional brain glucose metabolism and reported that regional metabolic measurements fell markedly with age in various frontal brain areas, including the anterior cingulate and the right supramarginal gyrus.

Finally, another novelty that this research introduces was showing how explainable artificial intelligence can point out the ROIs that are used to differentiate between healthy controls and patients. The post hoc explainability method SHAP was able to provide the most significant ROIs that were aligned with the statistical test results. Thus, it is important to make use of artificial intelligence models that are able to capture patterns in the data that are multi-variate and non-linear. We can even conclude that the model XGBoost and SHAP explainability were able to provide ROIs significantly aligned with the literature. SHAP outlined the accumbens, posterior cingulate, thalamus, pallidum, putamen, and caudate in the top 10 most significant ROIs used to diagnose patients. The aforementioned ROIs have been also reported by Quade's Test of Non-parametric

ANCOVA when the grouping factor is cohort(patient vs healthy control). Moreover, the global explainability method PDP enables us to investigate the individual effects of ROIs on dependent factors, the probability of being diagnosed with Schizophrenia. For instance, PDP reported that when the lateralization index value increases in Pallidum and exceeds threshold 0, the probability of being diagnosed with Schizophrenia increases. In other words, when the dopamine lateralization bias transitioned from right to left, the probability of being diagnosed with Schizophrenia increases. Regarding this, we can conclude that each ROI has a specific threshold for the lateralization index to sustain a healthy state of mind.

4.1 Limitations and Future Work

The small number of individuals both in healthy and patient cohorts, and the non-normal distribution of Ki values were the main limitations of this research to apply well-known methodologies in the literature. Less number of samples is disadvantageous for both artificial intelligence models to generalize and capture the underlying pattern behind data, and the production of precise measurements by the statistical methods. In future work, the patient cohort can be investigated in detail by taking the responder and non-responder groups into consideration. Additionally, taking the non-normal distribution of the data advanced normalization techniques and statistical approaches may be applied. Finally, more advanced deep learning or artificial intelligence models can be customized to work with PET imaging data.

References

Abedelahi, Ali et al. (2013). "Morphometric and volumetric study of caudate and putamen nuclei in normal individuals by MRI: effect of normal aging, gender and hemispheric differences". In: *Polish journal of radiology* 78.3, p. 7.

Albin, Roger L, Anne B Young, and John B Penney (1989). "The functional anatomy of basal ganglia disorders". In: *Trends in neurosciences* 12.10, pp. 366–375.

Aly-Mahmoud, Mayada et al. (2017). "Role of anterior cingulate cortex in instrumental learning: blockade of dopamine D1 receptors suppresses overt but not covert learning". In: *Frontiers in Behavioral Neuroscience* 11, p. 82.

Ardila, Alfredo, Byron Bernal, and Monica Rosselli (2016). "How localized are language brain areas? A review of Brodmann areas involvement in oral language". In: *Archives of Clinical Neuropsychology* 31.1, pp. 112–122.

Arias-Carrión, Óscar and Ernst Pöppel (2007). "Dopamine, learning, and reward-seeking behavior". In: *Acta neurobiologiae experimentalis* 67.4, pp. 481–488.

Bäckman, Lars et al. (2000). "Age-related cognitive deficits mediated by changes in the striatal dopamine system". In: *American Journal of Psychiatry* 157.4, pp. 635–637.

Baker, Justin T et al. (2014). "Disruption of cortical association networks in schizophrenia and psychotic bipolar disorder". In: *JAMA psychiatry* 71.2, pp. 109–118.

Barta, Patrick E et al. (1990). "Auditory hallucinations and smaller superior temporal gyral volume in schizophrenia." In: *The American journal of psychiatry*.

Bose, Subrata K et al. (2008). "Classification of schizophrenic patients and healthy controls using [18F] fluorodopa PET imaging". In: *Schizophrenia research* 106.2-3, pp. 148–155.

Calabria, Ferdinando et al. (2012). "Molecular imaging of brain tumors with 18F-DOPA PET and PET/CT". In: *Nuclear medicine communications* 33.6, pp. 563–570.

Cangür, Şengül, Mehmet Ali Sungur, and Handan Ankarali (2018). "The methods used in nonparametric covariance analysis". In: *Duzce Medical Journal* 20.1, pp. 1–6.

Chen, Tianqi and Carlos Guestrin (2016a). "XGBoost: A Scalable Tree Boosting System". In: *Proceedings of the 22nd ACM SIGKDD International Conference on Knowledge Discovery and Data Mining*. KDD '16. San Francisco, California, USA: ACM, pp. 785–794. ISBN: 978-1-4503-4232-2. DOI: 10.1145/2939672.2939785. URL: http://doi.acm.org/10.1145/2939672.2939785.

— (2016b). "Xgboost: A scalable tree boosting system". In: *Proceedings of the 22nd acm sigkdd international conference on knowledge discovery and data mining*, pp. 785–794.

Choi, Jung-Seok et al. (2005). "Decreased caudal anterior cingulate gyrus volume and positive symptoms in schizophrenia". In: *Psychiatry Research: Neuroimaging* 139.3, pp. 239–247.

Conover, William Jay (1999). *Practical nonparametric statistics*. Vol. 350. john wiley & sons.

Cools, Roshan et al. (2008). "Working memory capacity predicts dopamine synthesis capacity in the human striatum". In: *Journal of Neuroscience* 28.5, pp. 1208–1212.

Craig, Arthur D (2002). "How do you feel? Interoception: the sense of the physiological condition of the body". In: *Nature reviews neuroscience* 3.8, pp. 655–666.

de la Fuente-Fernández, Raúl et al. (2000). "Nigrostriatal dopamine system and motor lateralization". In: *Behavioural Brain Research* 112.1, pp. 63–68. ISSN: 0166-4328. DOI: https://doi.org/10.1016/S0166-4328(00)00165-0. URL: https://www.sciencedirect.com/science/article/pii/S0166432800001650.

DeRamus, Thomas P et al. (2020). "Covarying structural alterations in laterality of the temporal lobe in schizophrenia: A case for source-based laterality". In: *NMR in Biomedicine* 33.6, e4294.

Desikan, Rahul S. et al. (2006). "An automated labeling system for subdividing the human cerebral cortex on MRI scans into gyral based regions of interest". In: *NeuroImage* 31.3, pp. 968–980. ISSN: 1053-8119. DOI: https://doi.org/10.1016/j.neuroimage.2006.01.021. URL: https://www.sciencedirect.com/science/article/pii/S1053811906000437.

Dyck, Christopher H van et al. (2002). "Age-related decline in dopamine transporters: analysis of striatal subregions, nonlinear effects, and hemispheric asymmetries". In: *The American journal of geriatric psychiatry* 10.1, pp. 36–43.

Elkashef, Ahmed M et al. (2000). "6-18F-DOPA PET study in patients with schizophrenia". In: *Psychiatry Research: Neuroimaging* 100.1, pp. 1–11.

Elston, Guy N and Laurence J Garey (2013). "The cytoarchitectonic map of Korbinian Brodmann: arealisation and circuit specialisation". In: *Microstructural Parcellation of the Human Cerebral Cortex: From Brodmann's Post-Mortem Map to in Vivo Mapping with High-Field Magnetic Resonance Imaging*. Springer, pp. 3–32.

Erixon-Lindroth, Nina et al. (2005). "The role of the striatal dopamine transporter in cognitive aging". In: *Psychiatry Research: Neuroimaging* 138.1, pp. 1–12.

Falkai, Peter et al. (1992). "Loss of sylvian fissure asymmetry in schizophrenia: a quantitative post mortem study". In: *Schizophrenia Research* 7.1, pp. 23–32.

Farde, Lars et al. (1990). "D2 dopamine receptors in neuroleptic-naive schizophrenic patients: a positron emission tomography study with [11C] raclopride". In: *Archives of General Psychiatry* 47.3, pp. 213–219.

Fiorenzato, Eleonora et al. (2021). "Asymmetric dopamine transporter loss affects cognitive and motor progression in Parkinson's disease". In: *Movement Disorders* 36.10, pp. 2303–2313.

Fowler, Joanna S and Alfred P Wolf (1989). "New directions in positron emission tomography". In: *Annual Reports in Medicinal Chemistry*. Vol. 24. Elsevier, pp. 277–286.

Friederici, Angela D (2017). "Evolution of the neural language network". In: *Psychonomic bulletin & review* 24, pp. 41–47.

Friston, Karl J (2002). "Dysfunctional connectivity in schizophrenia". In: *World Psychiatry* 1.2, p. 66.

Fuertinger, Stefan et al. (2018). "Dopamine drives left-hemispheric lateralization of neural networks during human speech". In: *Journal of Comparative Neurology* 526.5, pp. 920–931.

Glick, Stanley D, David Alan Ross, and Lindsay B Hough (1982). "Lateral asymmetry of neurotransmitters in human brain". In: *Brain research* 234.1, pp. 53–63.

Goldstein, Alex et al. (2015). "Peeking inside the black box: Visualizing statistical learning with plots of individual conditional expectation". In: *journal of Computational and Graphical Statistics* 24.1, pp. 44–65.

Greenstein, Deanna et al. (2012). "Using multivariate machine learning methods and structural MRI to classify childhood onset schizophrenia and healthy controls". In: *Frontiers in psychiatry* 3, p. 53.

Guo, Gongde et al. (2003). "KNN model-based approach in classification". In: *On The Move to Meaningful Internet Systems 2003: CoopIS, DOA, and ODBASE: OTM Confederated International Conferences, CoopIS, DOA, and ODBASE 2003, Catania, Sicily, Italy, November 3-7, 2003. Proceedings*. Springer, pp. 986–996.

Hardy, SG Patrick (1985). "Analgesia elicited by prefrontal stimulation". In: *Brain research* 339.2, pp. 281–284.

Harms, Michael P et al. (2007). "Thalamic shape abnormalities in individuals with schizophrenia and their nonpsychotic siblings". In: *Journal of Neuroscience* 27.50, pp. 13835–13842.

Hay, S et al. (2017). "Global, regional, and national incidence, prevalence, and years lived with disability for 328 diseases and injuries for 195 countries, 1990–2016: a systematic analysis for the Global Burden of Disease Study 2016". In: *Lancet* 390.10100.

Hietala, Jarmo, Erkka Syvälahti, Harry Vilkman, et al. (1999). "Depressive symptoms and presynaptic dopamine function in neuroleptic-naive schizophrenia". In: *Schizophrenia research* 35.1, pp. 41–50.

Hietala, Jarmo, Erkka Syvälahti, Klaus Vuorio, et al. (1995). "Presynaptic dopamine function in striatum of neuroleptic-naive schizophrenic patients." In: *Lancet (London, England)* 346.8983, pp. 1130–1131.

Hilker, Rikke et al. (2018). "Heritability of schizophrenia and schizophrenia spectrum based on the nationwide Danish twin register". In: *Biological psychiatry* 83.6, pp. 492–498.

Hirvonen, Jussi et al. (2006). "Brain dopamine D 1 receptors in twins discordant for schizophrenia". In: *American Journal of Psychiatry* 163.10, pp. 1747–1753.

Hjorthøj, Carsten et al. (2017). "Years of potential life lost and life expectancy in schizophrenia: a systematic review and meta-analysis". In: *The Lancet Psychiatry* 4.4, pp. 295–301.

Hoegerle, Stefan et al. (2001). "Whole-body 18F dopa PET for detection of gastrointestinal carcinoid tumors". In: *Radiology* 220.2, pp. 373–380.

Hokama, Hiroto et al. (1995). "Caudate, putamen, and globus pallidus volume in schizophrenia: a quantitative MRI study". In: *Psychiatry Research: Neuroimaging* 61.4, pp. 209–229.

Hornykiewicz, OLEH (1966). "DOPAMINE (3-HYDROXYTYRAMINE) AND BRAIN FUNCTION". In: *Pharmacological Reviews* 18.2, pp. 925–964. ISSN: 0031-6997. eprint: https://pharmrev.aspetjournals.org/content/18/2/925.full.pdf. URL: https://pharmrev.aspetjournals.org/content/18/2/925.

Hugdahl, Kenneth et al. (2008). "Auditory hallucinations in schizophrenia: the role of cognitive, brain structural and genetic disturbances in the left temporal lobe". In: *Frontiers in Human Neuroscience*, p. 6.

Hwang, Kai et al. (2017). "The human thalamus is an integrative hub for functional brain networks". In: *Journal of Neuroscience* 37.23, pp. 5594–5607.

Ibrahim, Christine et al. (2019). "The insula: a brain stimulation target for the treatment of addiction". In: *Frontiers in pharmacology* 10, p. 720.

Insel, Thomas R (2010). "Rethinking schizophrenia". In: *Nature* 468.7321, pp. 187–193.

Ismail, Dunia and Khalid Hussain (2010). "Role of 18F-DOPA PET/CT imaging in congenital hyperinsulinism". In: *Reviews in endocrine and metabolic disorders* 11, pp. 165–169.

Jalili, Mahdi et al. (2010). "Attenuated asymmetry of functional connectivity in schizophrenia: A high-resolution EEG study". In: *Psychophysiology* 47.4, pp. 706–716.

Jiang, Yanbo, Mary H Patton, and Stanislav S Zakharenko (2021). "A case for thalamic mechanisms of schizophrenia: perspective from modeling 22q11. 2 deletion syndrome". In: *Frontiers in Neural Circuits*, p. 140.

Kalivas, Peter W and Nora D Volkow (2005). "The neural basis of addiction: a pathology of motivation and choice". In: *American Journal of Psychiatry* 162.8, pp. 1403–1413.

Katuwal, Gajendra Jung and Robert Chen (2016). "Machine learning model interpretability for precision medicine". In: *arXiv preprint arXiv:1610.09045*.

Koch, Giacomo et al. (2008). "Connectivity between posterior parietal cortex and ipsilateral motor cortex is altered in schizophrenia". In: *Biological psychiatry* 64.9, pp. 815–819.

Kringelbach, Morten L (2005). "The human orbitofrontal cortex: linking reward to hedonic experience". In: *Nature reviews neuroscience* 6.9, pp. 691–702.

Kutlu, Munir Gunes et al. (2021). "Dopamine release in the nucleus accumbens core signals perceived saliency". In: *Current Biology* 31.21, 4748–4761.e8. ISSN: 0960-9822. DOI: https://doi.org/10.1016/j.cub.2021.08.052. URL: https://www.sciencedirect.com/science/article/pii/S096098222101188X.

Libero, Lauren E et al. (2015). "Multimodal neuroimaging based classification of autism spectrum disorder using anatomical, neurochemical, and white matter correlates". In: *Cortex* 66, pp. 46–59.

Lichtenstein, Paul et al. (2009). "Common genetic determinants of schizophrenia and bipolar disorder in Swedish families: a population-based study". In: *The Lancet* 373.9659, pp. 234–239.

Linear, ICBM (n.d.). *Average Brain (ICBM152) Stereotaxic Registration Model*.

Loh, Hui Wen et al. (2022). "Application of explainable artificial intelligence for healthcare: A systematic review of the last decade (2011–2022)". In: *Computer Methods and Programs in Biomedicine*, p. 107161.

Lundberg, Scott M and Su-In Lee (2017). "A unified approach to interpreting model predictions". In: *Advances in neural information processing systems* 30.

Luo, Xingguang et al. (2019). "Putamen gray matter volumes in neuropsychiatric and neurodegenerative disorders". In: *World journal of psychiatry and mental health research* 3.1.

Mamah, Daniel et al. (2007). "Structural analysis of the basal ganglia in schizophrenia". In: *Schizophrenia research* 89.1-3, pp. 59–71.

Marinescu, Razvan et al. (2019). "BrainPainter: A software for the visualisation of brain structures, biomarkers and associated pathological processes". In: *arXiv preprint arXiv:1905.08627*.

Marinescu, Răzvan V et al. (2019). "BrainPainter: A software for the visualisation of brain structures, biomarkers and associated pathological processes". In: *Multimodal Brain Image Analysis and Mathematical Foundations of Computational Anatomy: 4th International Workshop, MBIA 2019, and 7th International Workshop, MFCA 2019, Held in Conjunction with MICCAI 2019, Shenzhen, China, October 17, 2019, Proceedings 4*. Springer, pp. 112–120.

McDonald, William M et al. (1991). "A magnetic resonance image study of age-related changes in human putamen nuclei." In: *Neuroreport* 2.1, pp. 57–60.

Mohammed, Ammar and Rania Kora (2023). "A comprehensive review on ensemble deep learning: Opportunities and challenges". In: *Journal of King Saud University-Computer and Information Sciences*.

Moreno-Küstner, Berta, Carlos Martin, and Loly Pastor (2018). "Prevalence of psychotic disorders and its association with methodological issues. A systematic review and meta-analyses". In: *PloS one* 13.4, e0195687.

Morrish, PK, GV Sawle, and DJ Brooks (1996). "An [18F] dopa–PET and clinical study of the rate of progression in Parkinson's disease". In: *Brain* 119.2, pp. 585–591.

Mozley, Lyn Harper et al. (2001). "Striatal dopamine transporters and cognitive functioning in healthy men and women". In: *American Journal of Psychiatry* 158.9, pp. 1492–1499.

Nicola, SM et al. (2005). "Nucleus accumbens dopamine release is necessary and sufficient to promote the behavioral response to reward-predictive cues". In: *Neuroscience* 135.4, pp. 1025–1033.

Nordio, Giovanna et al. (2023). "An automatic analysis framework for FDOPA PET neuroimaging". In: *Journal of Cerebral Blood Flow & Metabolism*, p. 0271678X231168687.

Numssen, Ole, Danilo Bzdok, and Gesa Hartwigsen (2021). "Functional specialization within the inferior parietal lobes across cognitive domains". In: *elife* 10, e63591.

Ocklenburg, Sebastian and Onur Güntürkün (2012). "Hemispheric asymmetries: the comparative view". In: *Frontiers in psychology* 3, p. 5.

Oke, Arvin et al. (1978). "Lateralization of norepinephrine in human thalamus". In: *Science* 200.4348, pp. 1411–1413.

Oke, Arvin F and Ralph N Adams (1987). "Elevated thalamic dopamine: a possible link to sensory dysfunctions in schizophrenia". In: *Schizophrenia Bulletin* 13.4, pp. 589–604.

Olguín, Hugo Juárez et al. (2016). "The role of dopamine and its dysfunction as a consequence of oxidative stress". In: *Oxidative medicine and cellular longevity* 2016, pp. 1–13.

Orlhac, Fanny et al. (2022). "A guide to ComBat harmonization of imaging biomarkers in multicenter studies". In: *Journal of Nuclear Medicine* 63.2, pp. 172–179.

Orru, Graziella et al. (2012). "Using support vector machine to identify imaging biomarkers of neurological and psychiatric disease: a critical review". In: *Neuroscience & Biobehavioral Reviews* 36.4, pp. 1140–1152.

Ortelli, Paola et al. (2018). "Asymmetric dopaminergic degeneration and attentional resources in Parkinson's disease". In: *Frontiers in neuroscience* 12, p. 972.

Paulus, Martin P and Murray B Stein (2006). "An insular view of anxiety". In: *Biological psychiatry* 60.4, pp. 383–387.

Pedregosa, F. et al. (2011). "Scikit-learn: Machine Learning in Python". In: *Journal of Machine Learning Research* 12, pp. 2825–2830.

Perez-Rando, Marta et al. (2022). "Alterations in the volume of thalamic nuclei in patients with schizophrenia and persistent auditory hallucinations". In: *NeuroImage: Clinical* 35, p. 103070.

Pergola, Giulio et al. (2015). "The role of the thalamus in schizophrenia from a neuroimaging perspective". In: *Neuroscience & Biobehavioral Reviews* 54, pp. 57–75.

Picchioni, Marco M and Robin M Murray (2007). "Schizophrenia". In: *BMJ* 335.7610, pp. 91–95. ISSN: 0959-8138. DOI: 10.1136/bmj.39227.616447.BE. eprint: https://www.bmj.com/content/335/7610/91.full.pdf. URL: https://www.bmj.com/content/335/7610/91.

Prasad, Asheeta A and Gavan P McNally (2019). "Ventral pallidum and alcohol addiction". In: *Neuroscience of Alcohol*. Elsevier, pp. 163–170.

Quade, Dana (1967). "Rank analysis of covariance". In: *Journal of the American Statistical Association* 62.320, pp. 1187–1200.

Rao, Naren P et al. (2010). "Clinical correlates of thalamus volume deficits in anti-psychotic-naive schizophrenia patients: A 3-Tesla MRI study". In: *Indian journal of psychiatry* 52.3, p. 229.

Raz, Naftali, Faith M Gunning, et al. (1997). "Selective aging of the human cerebral cortex observed in vivo: differential vulnerability of the prefrontal gray matter." In: *Cerebral cortex (New York, NY: 1991)* 7.3, pp. 268–282.

Raz, Naftali, Ivan J Torres, and James D Acker (1995). "Age, gender, and hemispheric differences in human striatum: a quantitative review and new data from in vivo MRI morphometry". In: *Neurobiology of learning and memory* 63.2, pp. 133–142.

Rentería, Miguel E (2012). "Cerebral asymmetry: a quantitative, multifactorial, and plastic brain phenotype". In: *Twin Research and Human Genetics* 15.3, pp. 401–413.

Ribeiro, Marco Tulio, Sameer Singh, and Carlos Guestrin (2016). "" Why should i trust you?" Explaining the predictions of any classifier". In: *Proceedings of the 22nd ACM SIGKDD international conference on knowledge discovery and data mining*, pp. 1135–1144.

Ribolsi, Michele et al. (2009). "Abnormal brain lateralization and connectivity in schizophrenia". In: *Reviews in the Neurosciences* 20.1, pp. 61–70.

Rosenblatt, Frank (1958). "The perceptron: a probabilistic model for information storage and organization in the brain." In: *Psychological review* 65.6, p. 386.

Rossor, M, N Garrett, and L Iversen (1980). "No evidence for lateral asymmetry of neurotransmitters in post-mortem human brain". In: *Journal of neurochemistry* 35.3, pp. 743–745.

Saha, Sukanta et al. (2005). "A systematic review of the prevalence of schizophrenia". In: *PLoS medicine* 2.5, e141.

Samanez-Larkin, Gregory R et al. (2013). "A thalamocorticostriatal dopamine network for psychostimulant-enhanced human cognitive flexibility". In: *Biological psychiatry* 74.2, pp. 99–105.

Schnider, Armin, Valerie Treyer, and Alfred Buck (2005). "The human orbitofrontal cortex monitors outcomes even when no reward is at stake". In: *Neuropsychologia* 43.3, pp. 316–323. ISSN: 0028-3932. DOI: https://doi.org/10.1016/j.neuropsychologia.2004.07.003. URL: https://www.sciencedirect.com/science/article/pii/S002839320400168X.

Schultz, Wolfram (2007). "Behavioral dopamine signals". In: *Trends in neurosciences* 30.5, pp. 203–210.

Smith, Kyle S et al. (2009). "Ventral pallidum roles in reward and motivation". In: *Behavioural brain research* 196.2, pp. 155–167.

Soares, Jair C and Robert B Innis (1999). "Neurochemical brain imaging investigations of schizophrenia". In: *Biological psychiatry* 46.5, pp. 600–615.

Sommer, Iris et al. (2001). "Handedness, language lateralisation and anatomical asymmetry in schizophrenia: meta-analysis". In: *The British Journal of Psychiatry* 178.4, pp. 344–351.

Sommer, Iris E et al. (2020). "The clinical course of schizophrenia in women and men—a nation-wide cohort study". In: *NPJ schizophrenia* 6.1, p. 12.

Stelzel, Christine et al. (2010). "Frontostriatal involvement in task switching depends on genetic differences in d2 receptor density". In: *Journal of Neuroscience* 30.42, pp. 14205–14212.

Suhara, Tetsuya et al. (1992). "D 1 dopamine receptor binding in mood disorders measured by positron emission tomography". In: *Psychopharmacology* 106, pp. 14–18.

Takao, Hidemasa et al. (2010). "Cerebral asymmetry in patients with schizophrenia: A voxel-based morphometry (VBM) and diffusion tensor imaging (DTI) study". In: *Journal of Magnetic Resonance Imaging* 31.1, pp. 221–226.

Toda, Mitsuru and Anissa Abi-Dargham (2007). "Dopamine hypothesis of schizophrenia: making sense of it all". In: *Current psychiatry reports* 9.4, pp. 329–336.

Toga, Arthur W and Paul M Thompson (2003). "Mapping brain asymmetry". In: *Nature Reviews Neuroscience* 4.1, pp. 37–48.

Torrey, E Fuller (2007). "Schizophrenia and the inferior parietal lobule". In: *Schizophrenia research* 97.1-3, pp. 215–225.

Van Haren, Neeltje EM et al. (2011). "Changes in cortical thickness during the course of illness in schizophrenia". In: *Archives of general psychiatry* 68.9, pp. 871–880.

Veronese, Mattia et al. (2021). "A potential biomarker for treatment stratification in psychosis: evaluation of an [18F] FDOPA PET imaging approach". In: *Neuropsychopharmacology* 46.6, pp. 1122–1132.

Volkow, Nora D et al. (1996). "PET evaluation of the dopamine system of the human brain". In: *Journal of Nuclear Medicine* 37.7, pp. 1242–1256.

Wagner, Gerd et al. (2015). "Structural and functional dysconnectivity of the front-thalamic system in schizophrenia: a DCM-DTI study". In: *Cortex* 66, pp. 35–45.

Wang, Yue et al. (1998). "Age-dependent decline of dopamine D1 receptors in human brain: A PET study". In: *Synapse* 30.1, pp. 56–61.

Wise, Roy A and Mykel A Robble (2020). "Dopamine and addiction". In: *Annual review of psychology* 71, pp. 79–106.

Zhang, Ruibin et al. (2015). "Disrupted brain anatomical connectivity in medication-naïve patients with first-episode schizophrenia". In: *Brain Structure and Function* 220, pp. 1145–1159.

Zhou, Ling et al. (2020). "Diffusion tensor imaging study of brain precentral gyrus and postcentral gyrus during normal brain aging process". In: *Brain and Behavior* 10.10, e01758.

Acknowledgments

I would like to express my gratitude and warmest thanks to my supervisor Prof. Mattia Veronese for his guidance and advice through the analysis and writing stages of this independent and creative thesis work. I would like to give special thanks to my co-supervisor Alessio Giacomel M.Sc. for his contribution, assistance, help, and cheerful attitude. Further, I also would like to indicate my appreciation to my other supervisor Giovanna Nordio Ph.D. for her contributions.